Cellular and Molecular Biophysics

Alessandra Fiorio Pla

UNIVERSITÀ DI TORINO

Department of Life Sciences and Systems Biology

CFU 5 LM Biotecnologie Industriali- 6 LM Fisica - A.A. 2023/24

Corso di laurea in LM Biotecnologie Industriali- LM Fisica

THE VERSATILITY AND UNIVERSALITY OF CALCIUM SIGNALLING

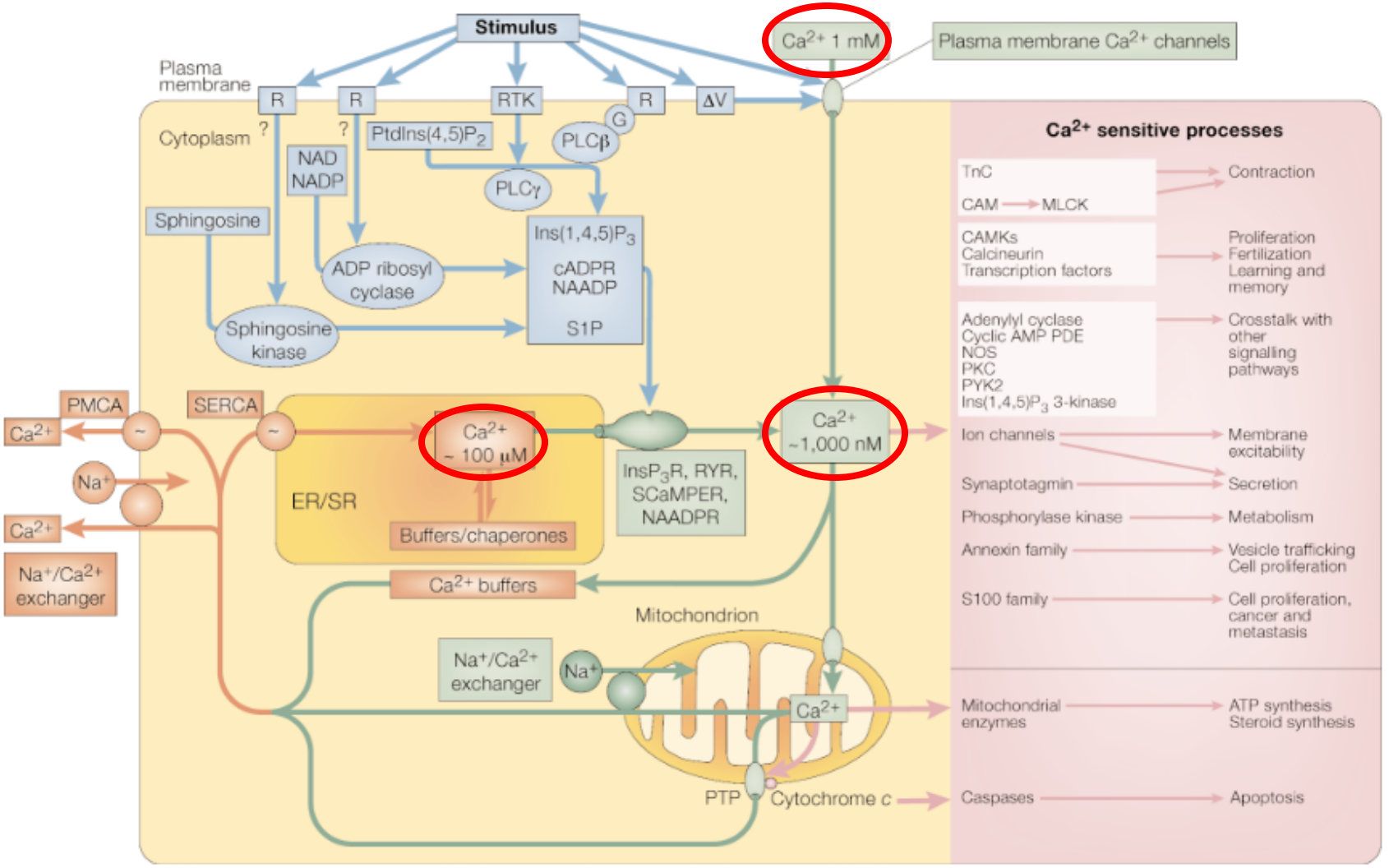

Berridge, M., Lipp, P. & Bootman, M., 2000

CALCIUM SIGNALING TOOLKIT

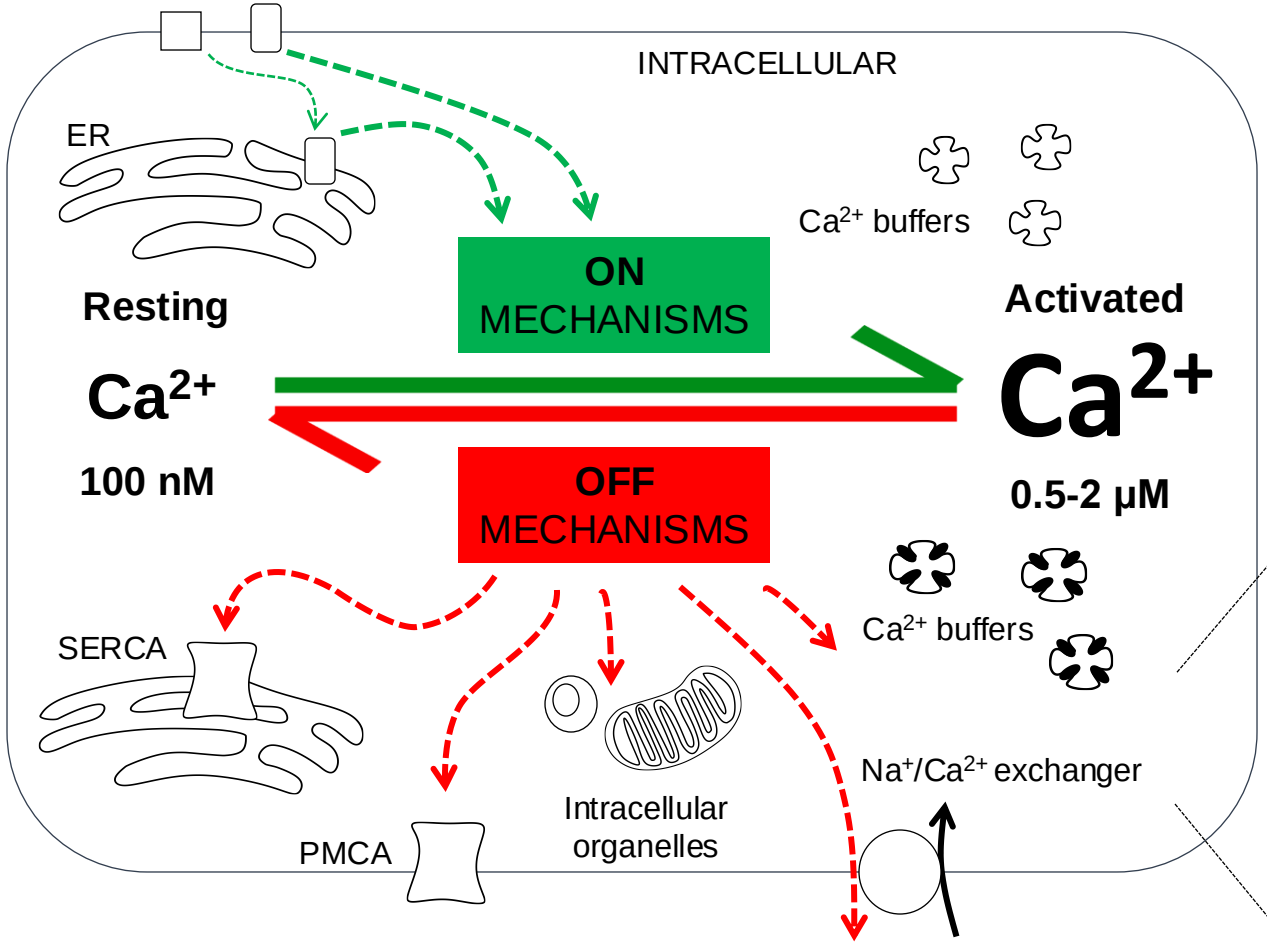

EXTRACELLULAR

Ca^{2+}

1-2 mM

CALCIUM TRANSIENT

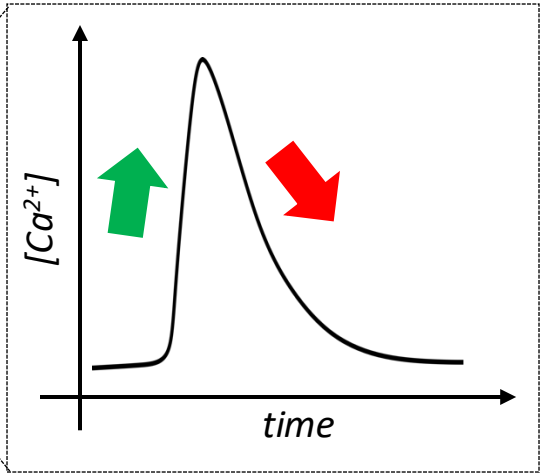

ON MECHANISMS

- Extracellular Ca^{2+} entry (ion channel)
- Intracellular Ca^{2+} release (Ca^{2+} stores)

OFF MECHANISMS

- Ca^{2+} buffers (calnexin, calsequestrin, calreticulin, …)
- Intracellular stores (ER, mitochondria, lysosomes, …)
- Na^{+}/Ca^{2+} exchanger and Ca^{2+} pumps (SERCA/PMCA)

OFF MECHANISMS

ON MECHANISMS

PMCA

↑ affinity

↓ capacity

SERCA

↓ affinity

↑ capacity

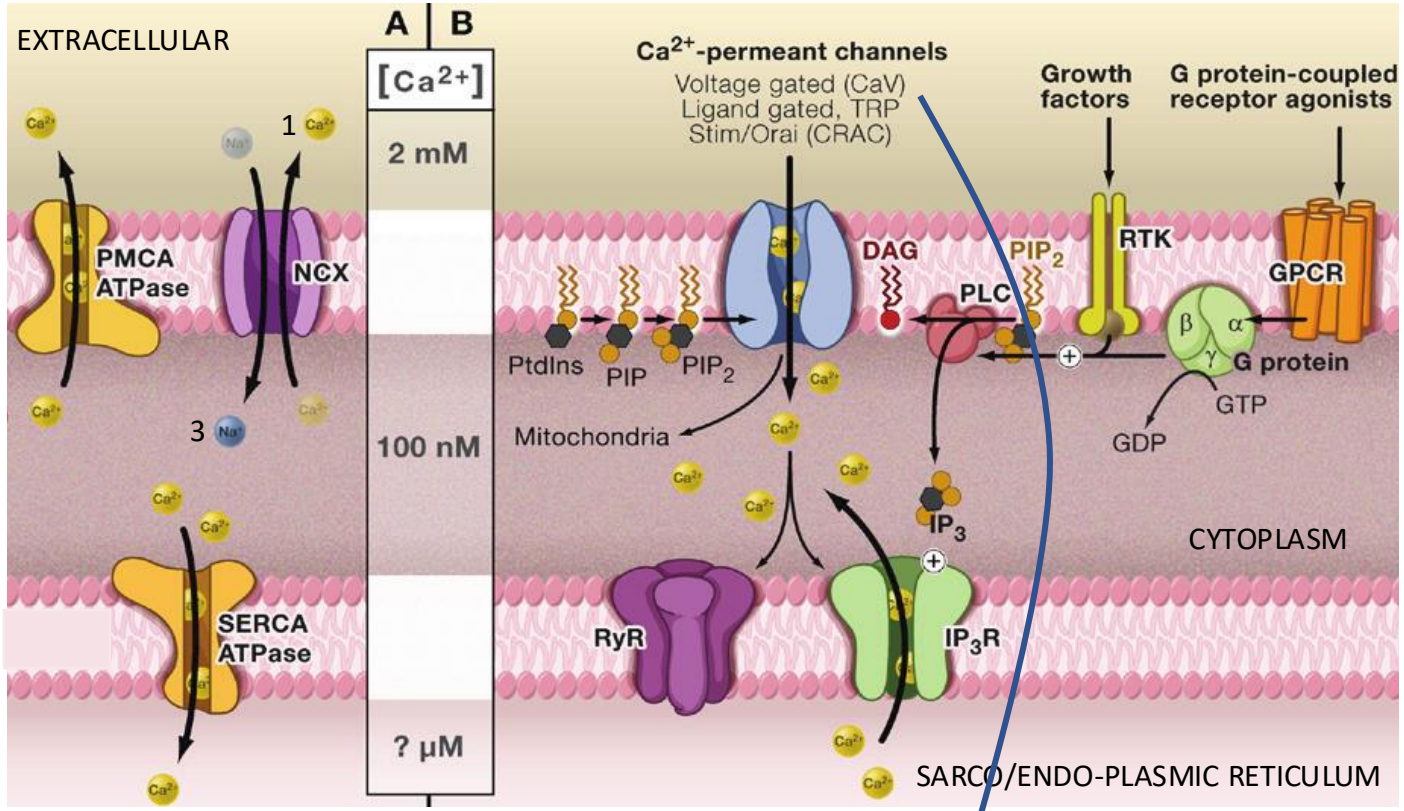

Modified from Clapham D., Cell *131, December 14, 2007 ©2007 Elsevier Inc.*

Ca^{2+} - permeable channels

- Voltage gated (CaV)
- Ligand gated (Ionotropic receptors, …)
- Mechano-gated (TRP, …)
- Store Operated Channel (**SOC**) (ORAI, TRPC1, …)

STORE OPERATED Ca^{2+} ENTRY (SOCE)

SOCE is the extracellular Ca^{2+} entry following the emptying of ER

Ca^{2+} levels in ER decrease as a result of three main events

1. activation of IP_3R/RyR receptors
2. blocking SERCA activity
3. pharmacology application (Ionomycin)

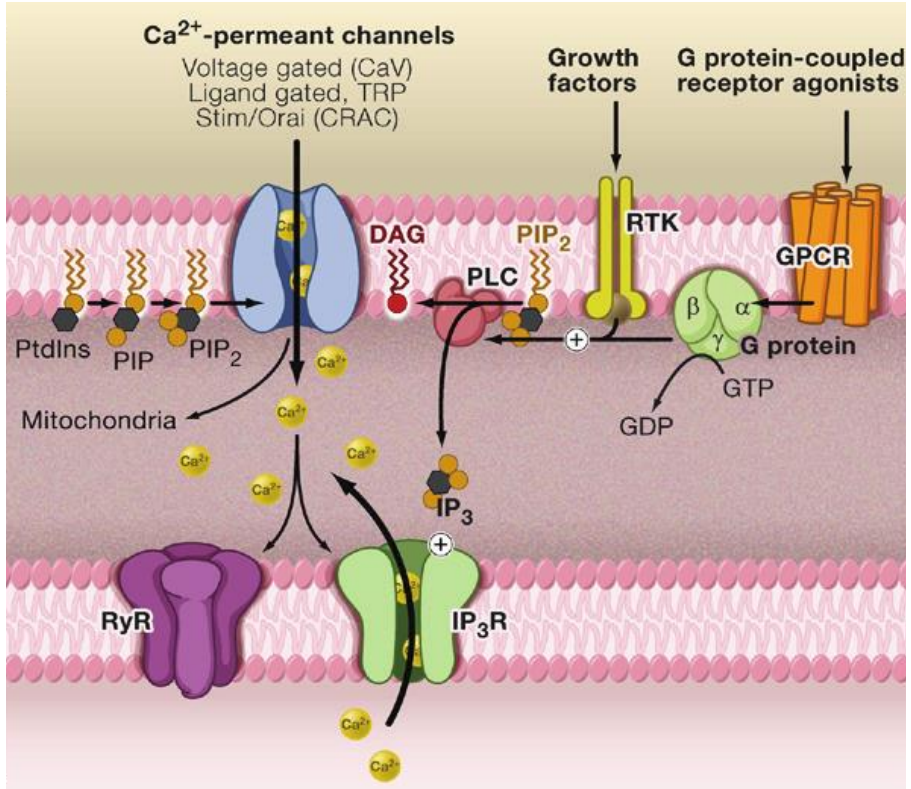

Modified from Clapham D., Cell *131, December 14, 2007 ©2007 Elsevier Inc.*

STORE OPERATED Ca^{2+} ENTRY (SOCE)

SOCE is the extracellular Ca^{2+} entry following the emptying of ER

Ca^{2+} levels in ER decrease as a result of three main events

1. activation of IP_3R/RyR receptors
2. **blocking SERCA activity**
3. pharmacology application (Ionomycin)

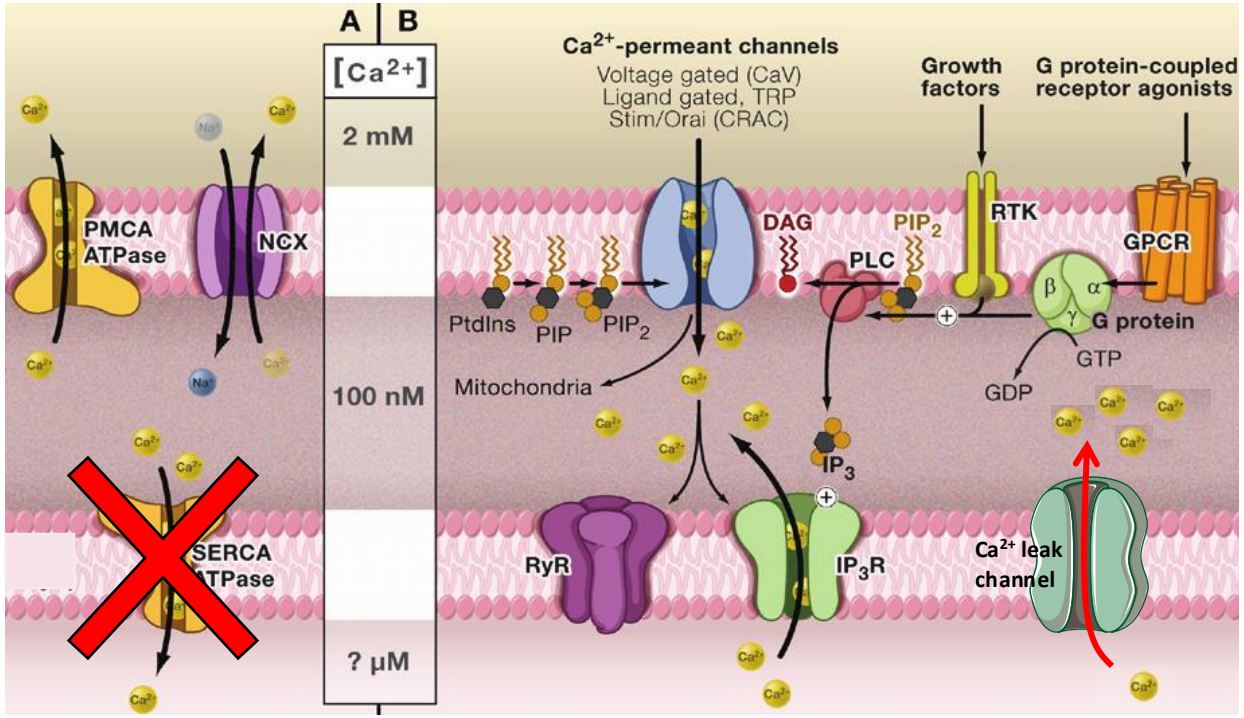

Modified from Clapham D., Cell *131, December 14, 2007 ©2007 Elsevier Inc.*

STORE OPERATED Ca^{2+} ENTRY (SOCE)

$[Ca^{2+}]_{ER}$ decrease causes extracellular Ca^{2+} entry through SOCE mechanism in order to restablish intracellular Ca^{2+} homeostasis

STIM is the calcium sensor in ER

(stromal interaction molecule)

STIM1 STIM2

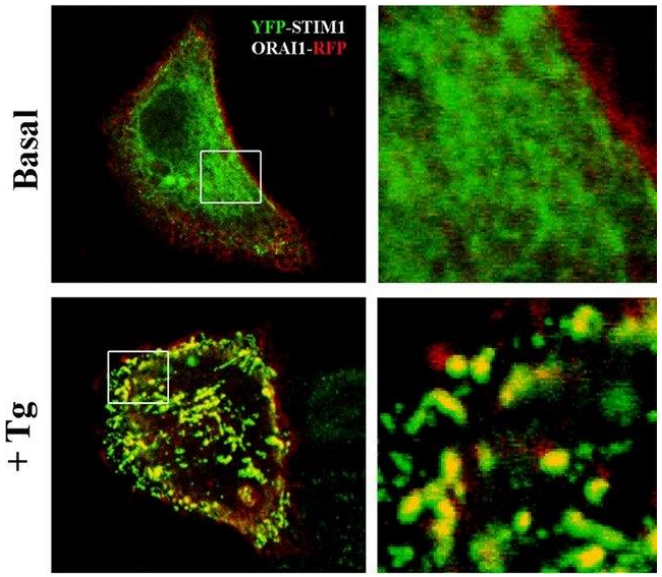

STIM1-ORAI1 complexes organize in ''puncta''

STIM1- TRPC1/3/6

I_{SOC}

store operated current

STIM1-ORAI1

I_{CRAC}

Ca^{2+} release activated current

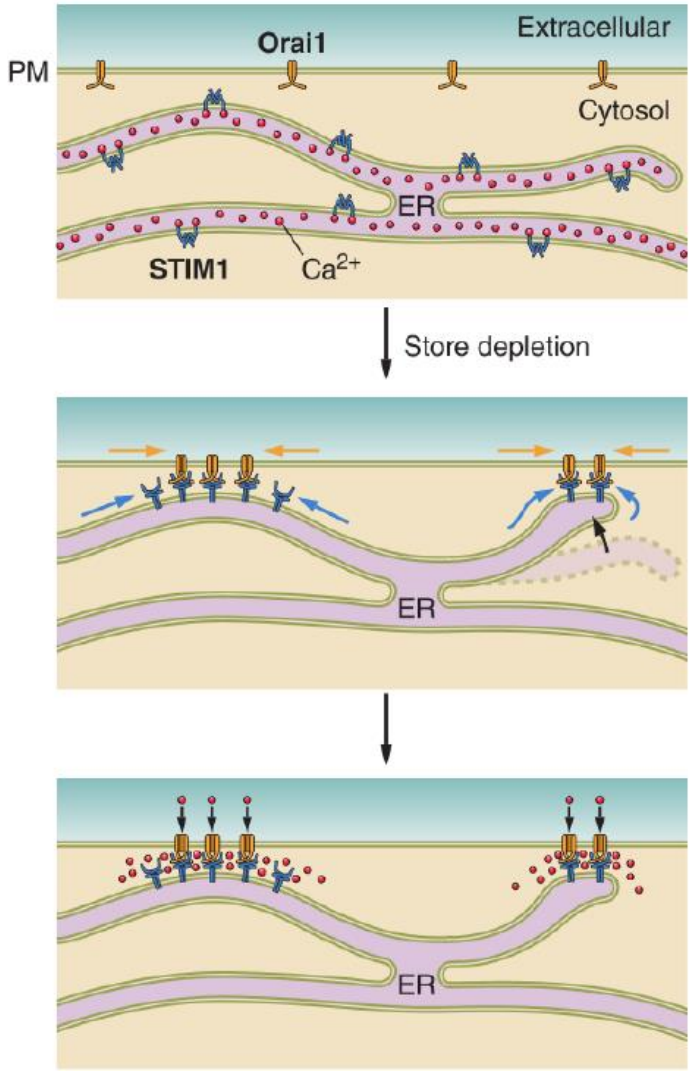

Prakriyan e Lewis, 2015

STORE OPERATED Ca^{2+} ENTRY (SOCE)

Ca^{2+} signals: examples of SOCE

blocking SERCA

TG: thapsigargin
CPA: ciclo piazonic acid

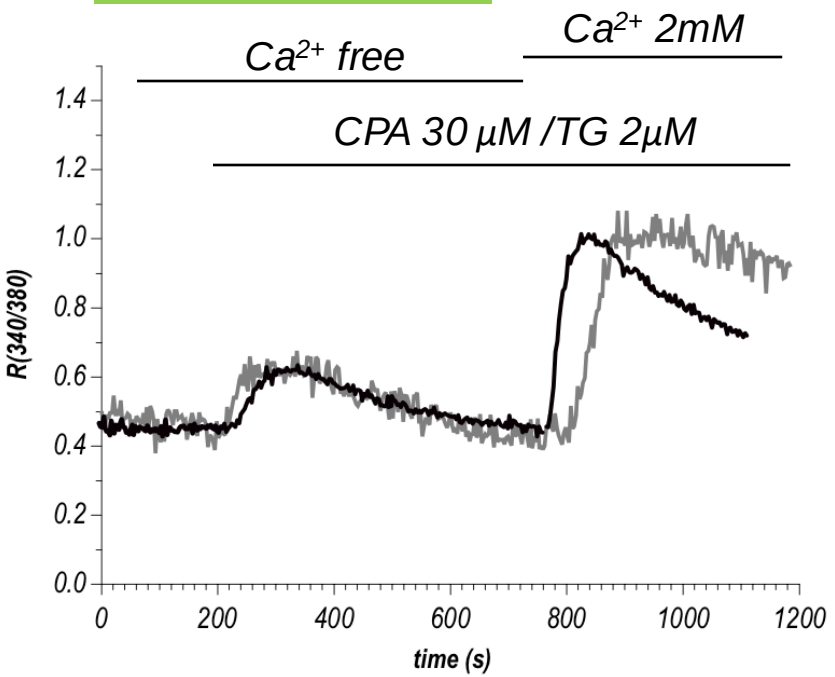

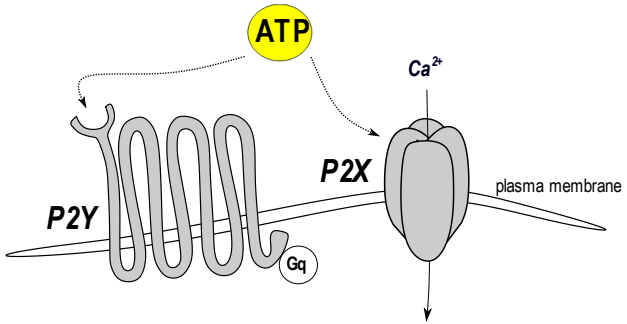

activating IP_3R

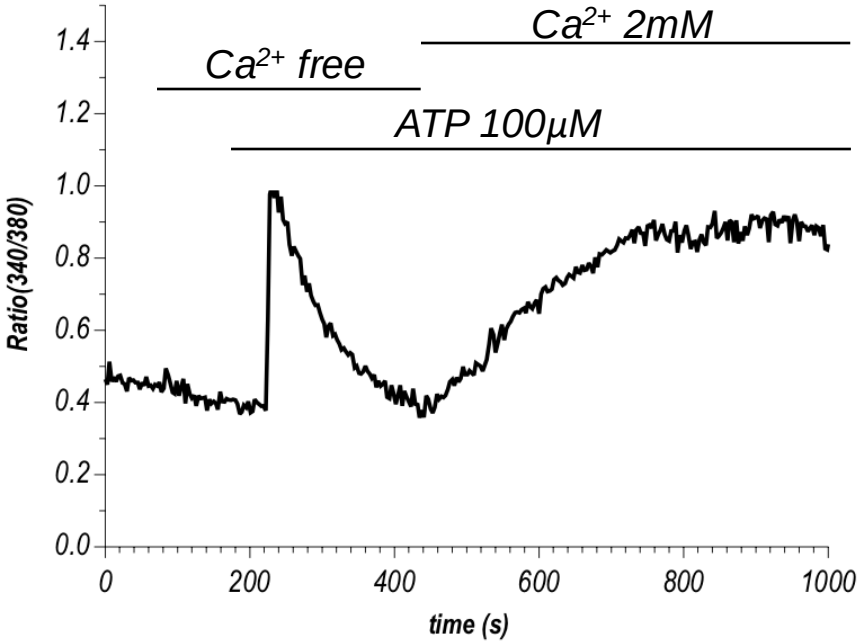

STORE OPERATED Ca^{2+} ENTRY (SOCE)

Ca^{2+} signals: examples of SOCE

activating IP_3R

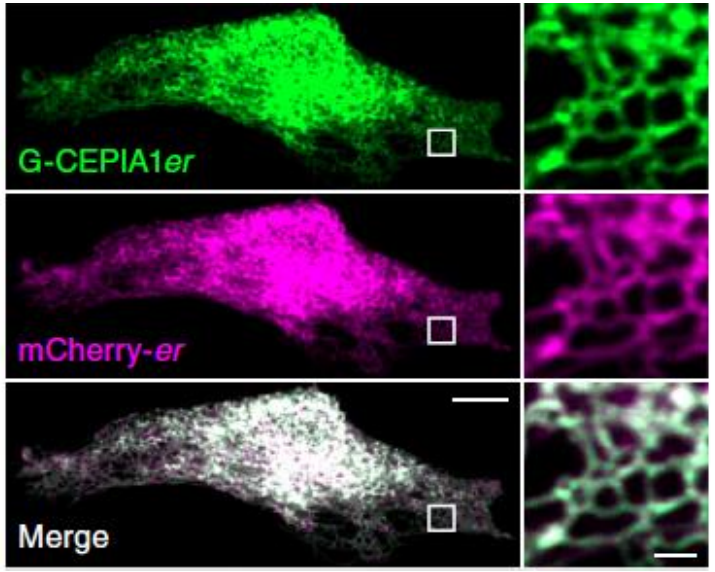

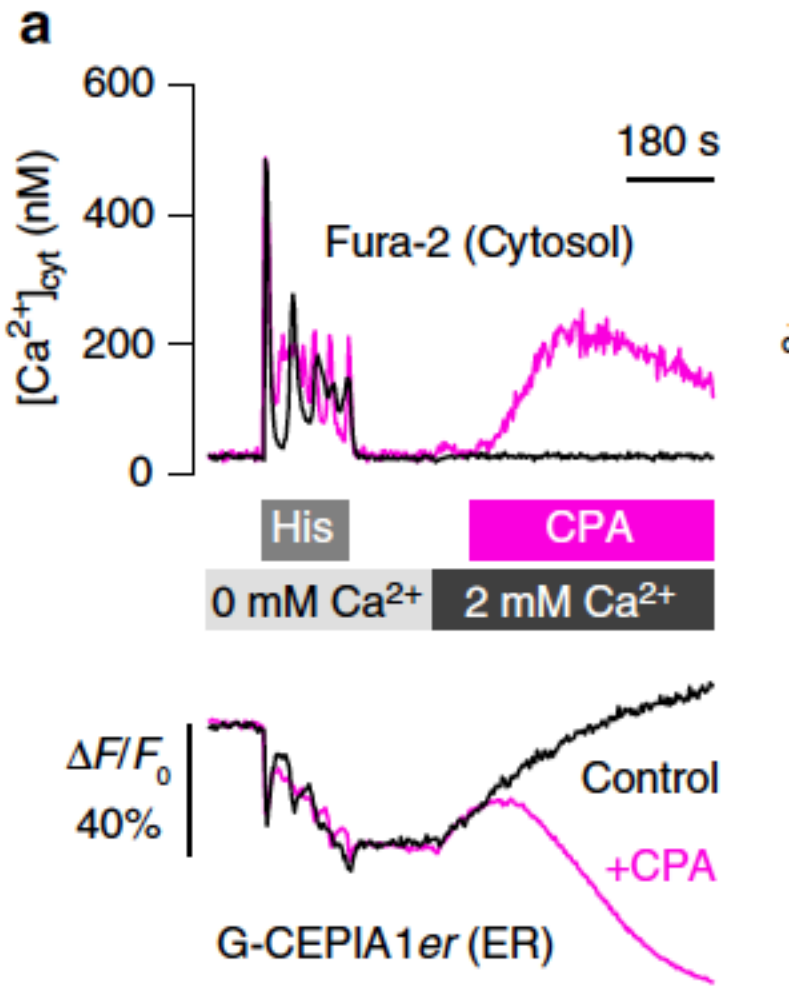

Ca^{2+}: ONE MESSENGER, MULTIPLE EFFECTS

Michael J. Berridge – www.cellsignallingbiology.org - 2012

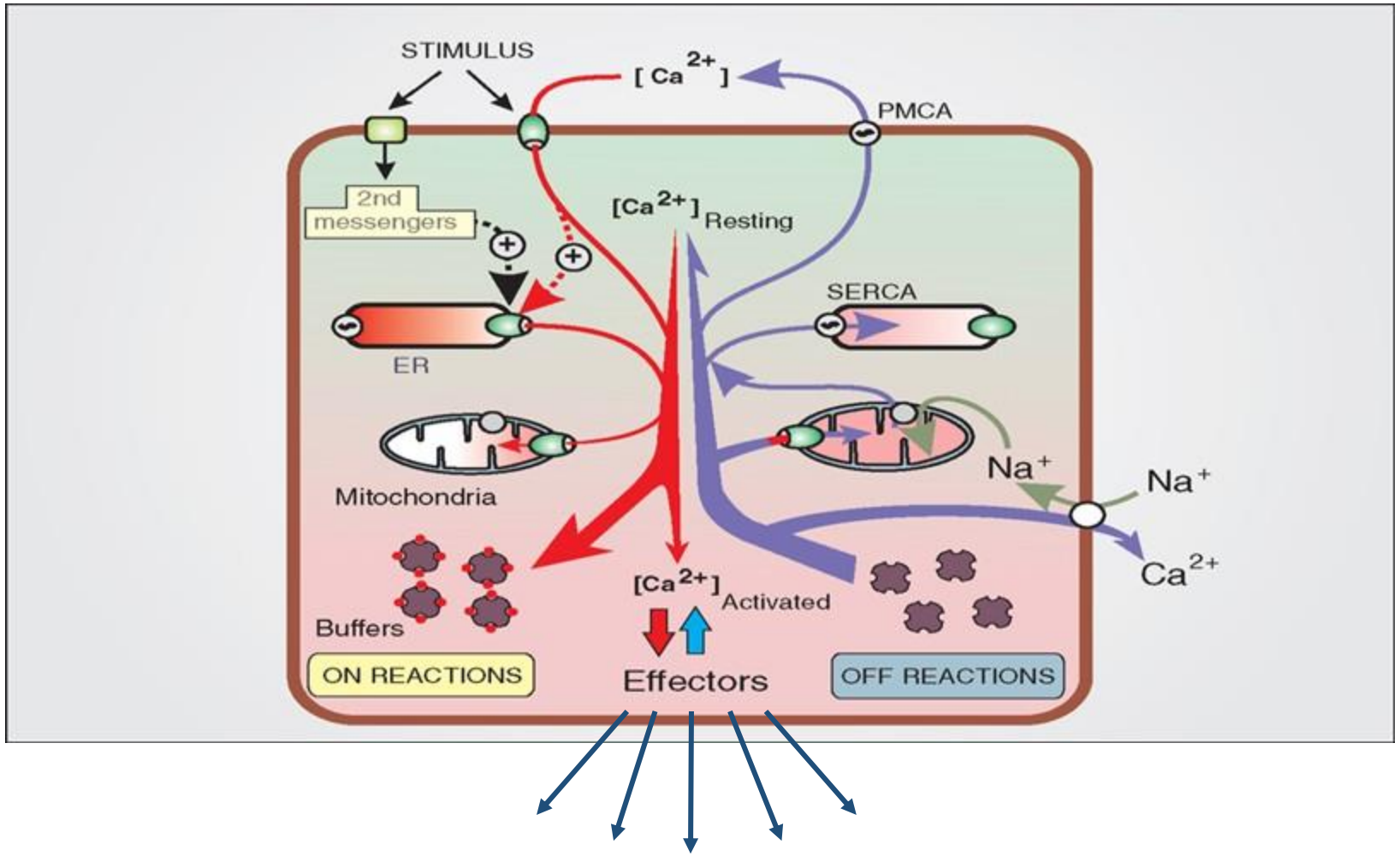

many functions

DECODIFICATION OF Ca^{2+} SIGNALS

space-time control of Ca^{2+} signals

1. AMPLITUDE

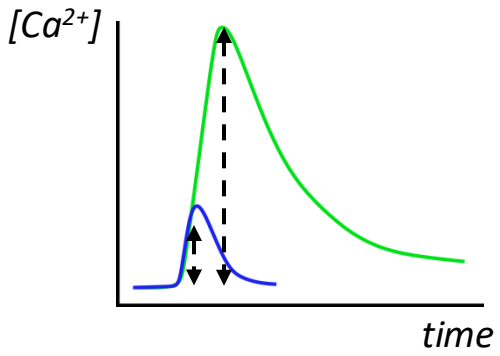

2. FREQUENCY

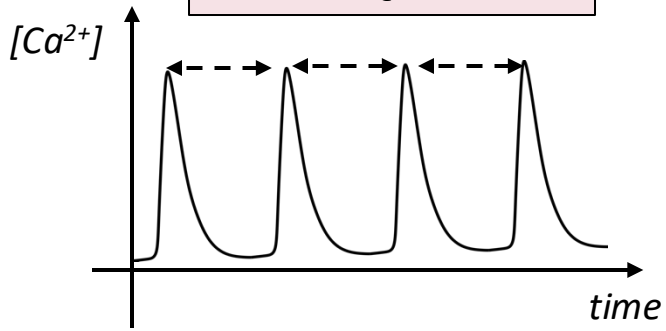

3. LOCALIZATION

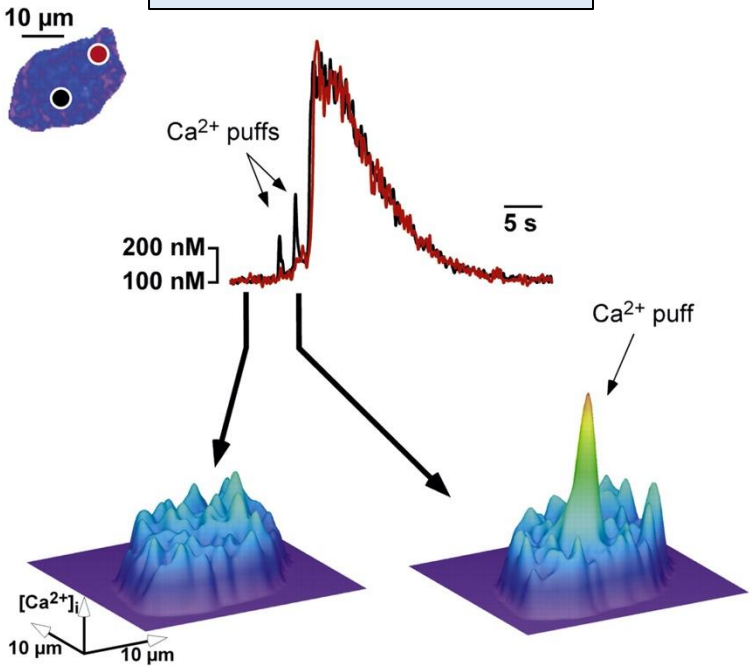

Martin D. Bootman, Peter Lipp, Michael J. Berridge

4. TIME

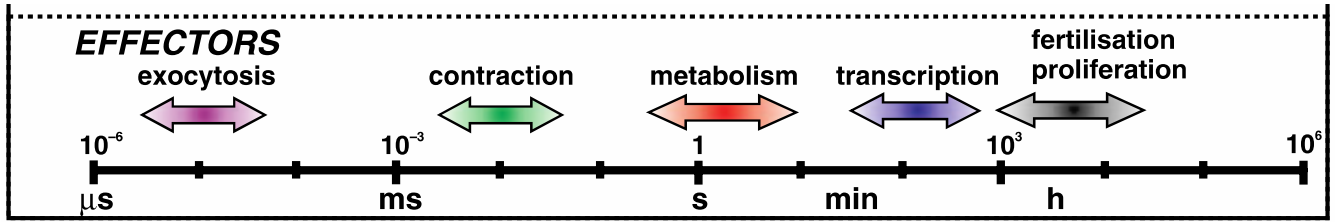

SPATIAL CONTROL

compartmentalization of Ca^{2+} signals allows the activation of different processes

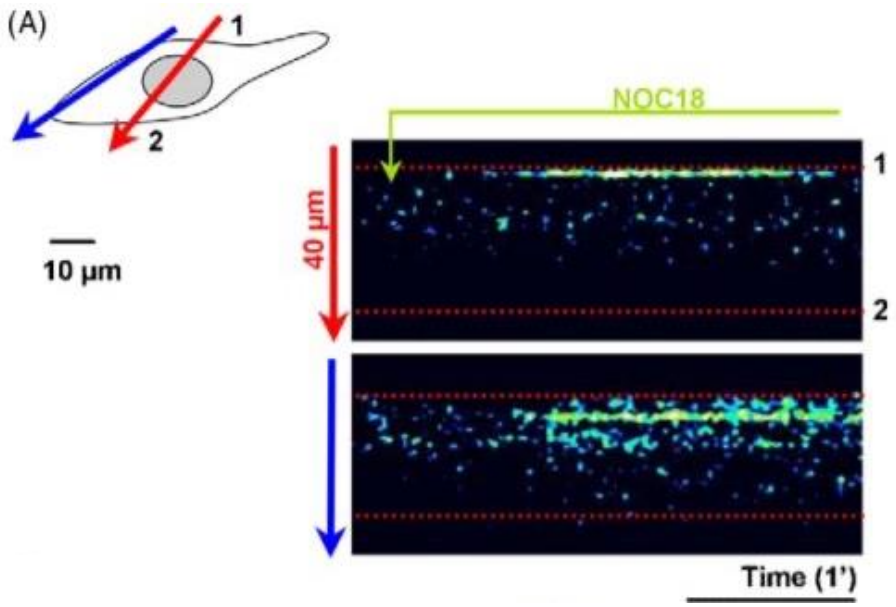

NO production requires increased [Ca^{2+}] close to the membrane

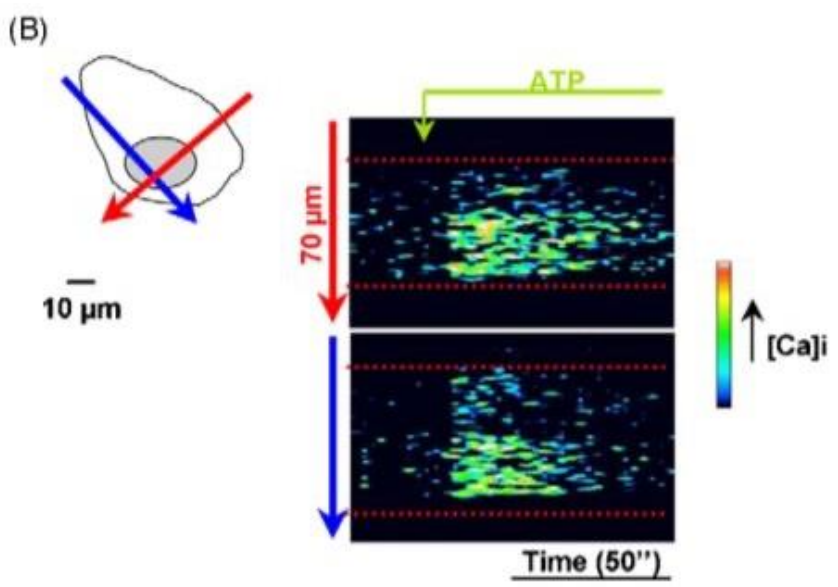

extracellular ATP induces wide intracellular [Ca^{2+}] increase

Tomatis C, Fiorio Pla A, Munaron L., Cell Calcium, 2007

TEMPORAL CONTROL

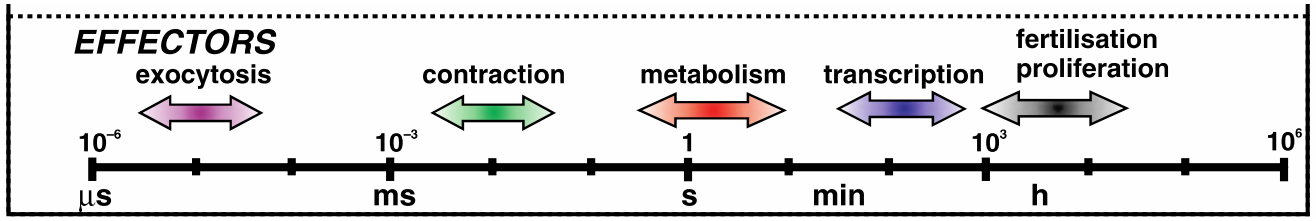

PERIODIC STIMULATION

high frequency

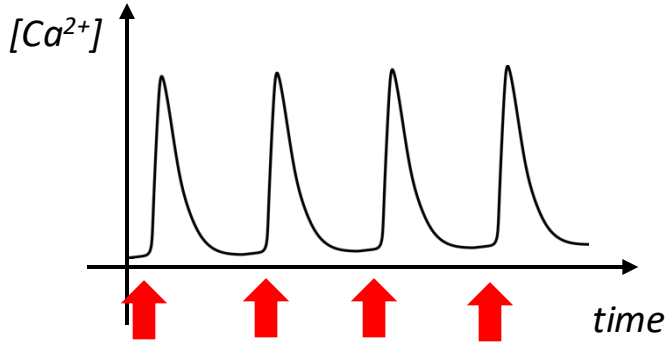

skeletal and cardiac cell contraction, synaptic transmission

CONTINUOUS STIMULATION

low frequency

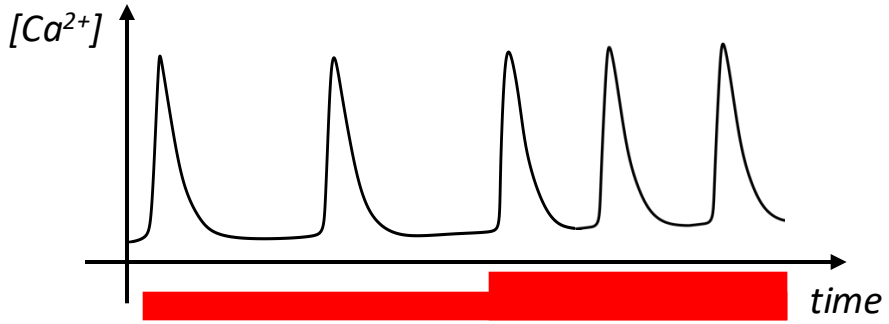

fertilization, fluid secretion, smooth muscle contraction, cell proliferation

long lasting intracellular Ca^{2+} increment → Ca^{2+} oscillations

SPATIO-TEMPORAL Ca^{2+} DYNAMICS OF FERTILIZATION

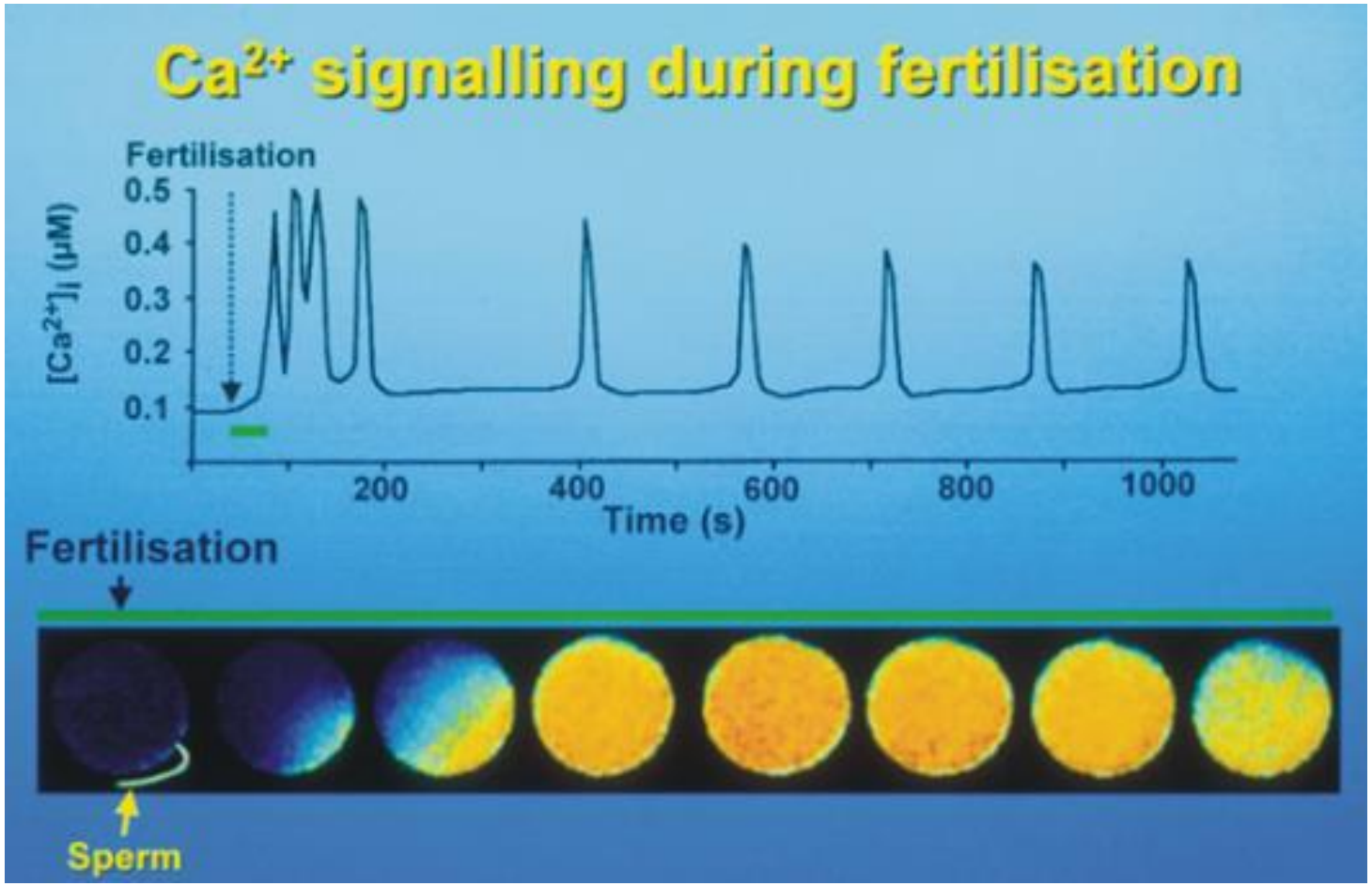

Michael J. Berridge – www.cellsignallingbiology.org - 2012

INTRA- and INTER CELLULAR Ca^{2+} SIGNALS

IP_3R and RyR are activated by Ca^{2+}

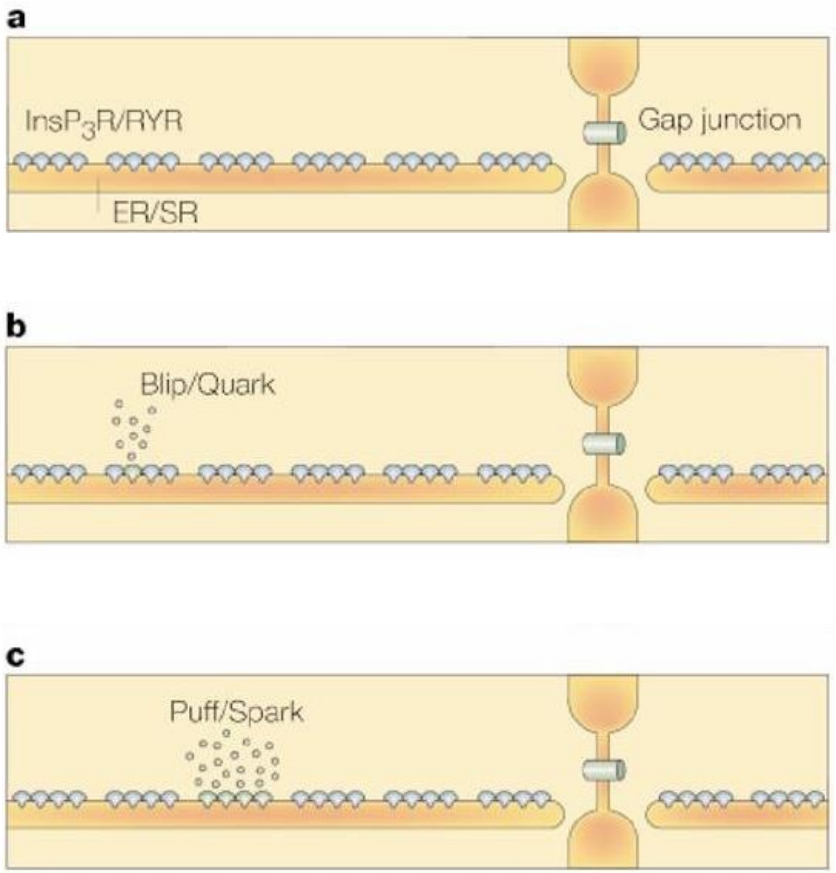

single channel
- BLIP (IP_3R)
- QUARK (RyR)

cluster
- PUFF (IP3R)
- SPARK (RyR)

Modified from Berridge, M., Lipp, P. & Bootman, M., 2000

from ELEMENTARY Ca^{2+} EVENTS…

… to CELL RESPONSE

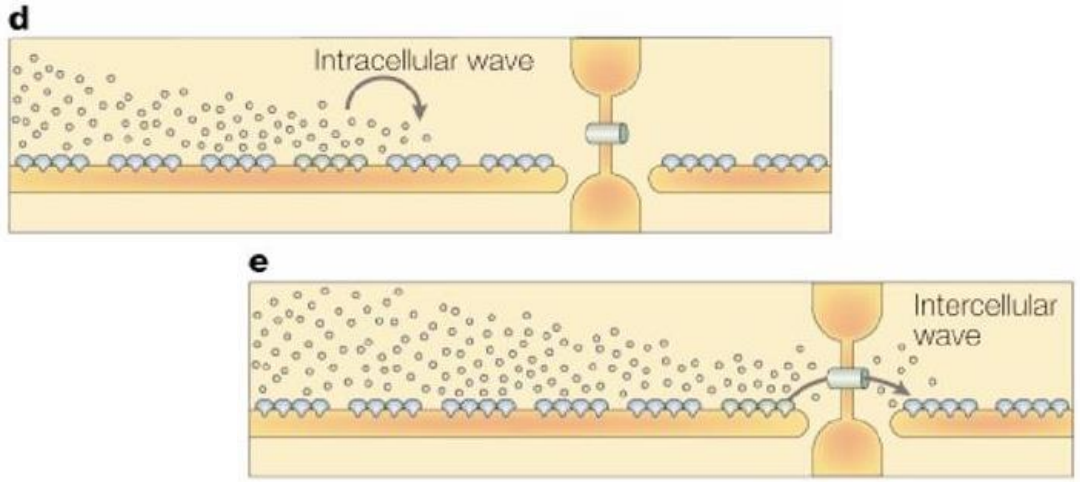

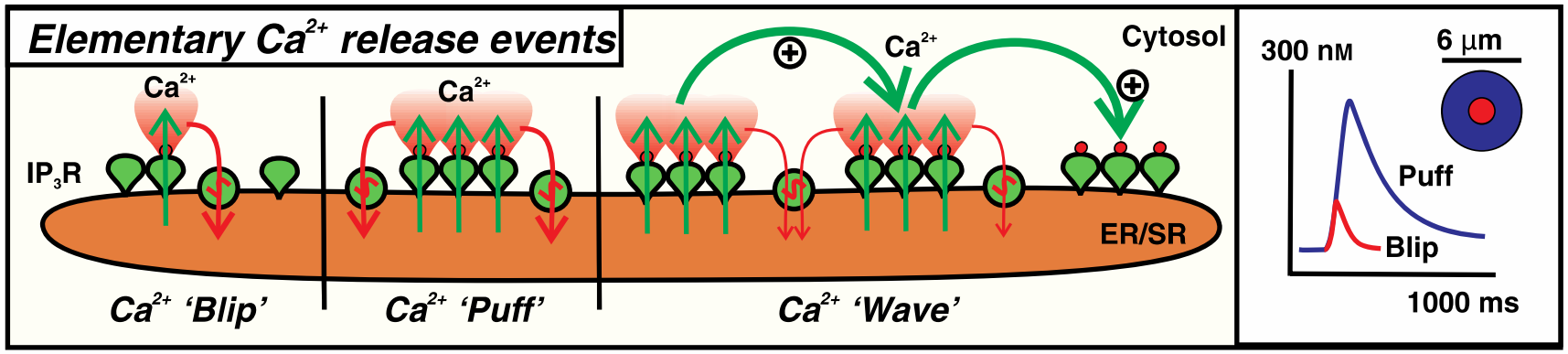

Modified from Alex J. Laude, Alec W. M. Simpson, 2009

Biphasic relationship between IP_3R and $[Ca^{2+}]$

ACTIVATION → ***IP_3R*** IP_3 and Ca^{2+}

ACTIVATION → ***RyR*** Ca^{2+} and cADP-ribose

(excitable cells)

NADP $\xrightarrow{CD38}$ cADP-r

NADP $\xrightarrow{CD38}$ NAADP

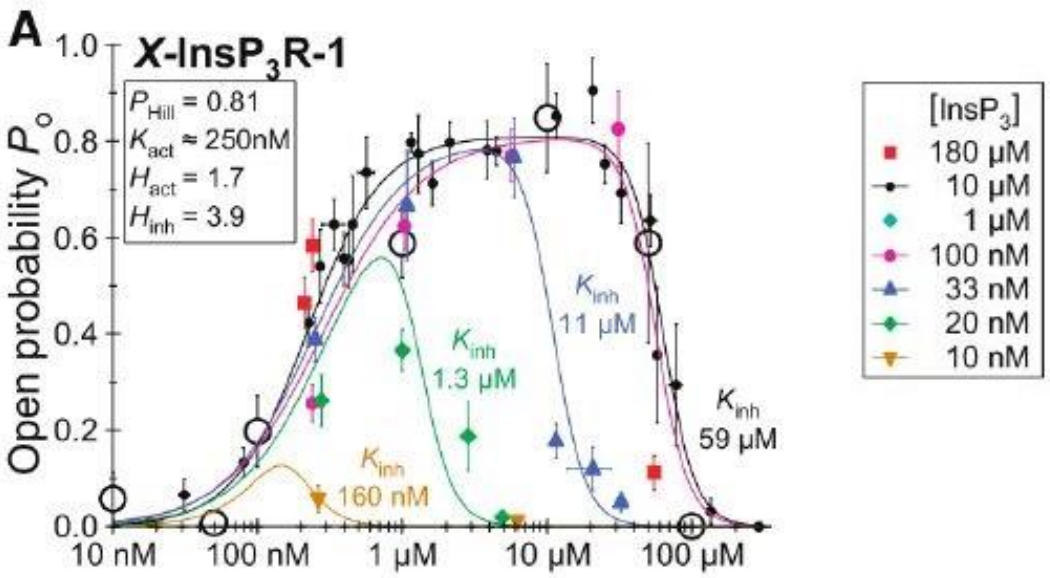

Foskett J.K. et al., Physiol Rev, 2007

→ Modified from Max et al., J Gen Physiol, 2001

physical Ca^{2+} compartments: MITOCHONDRIA

Mitochondrial Ca^{2+} uniporter

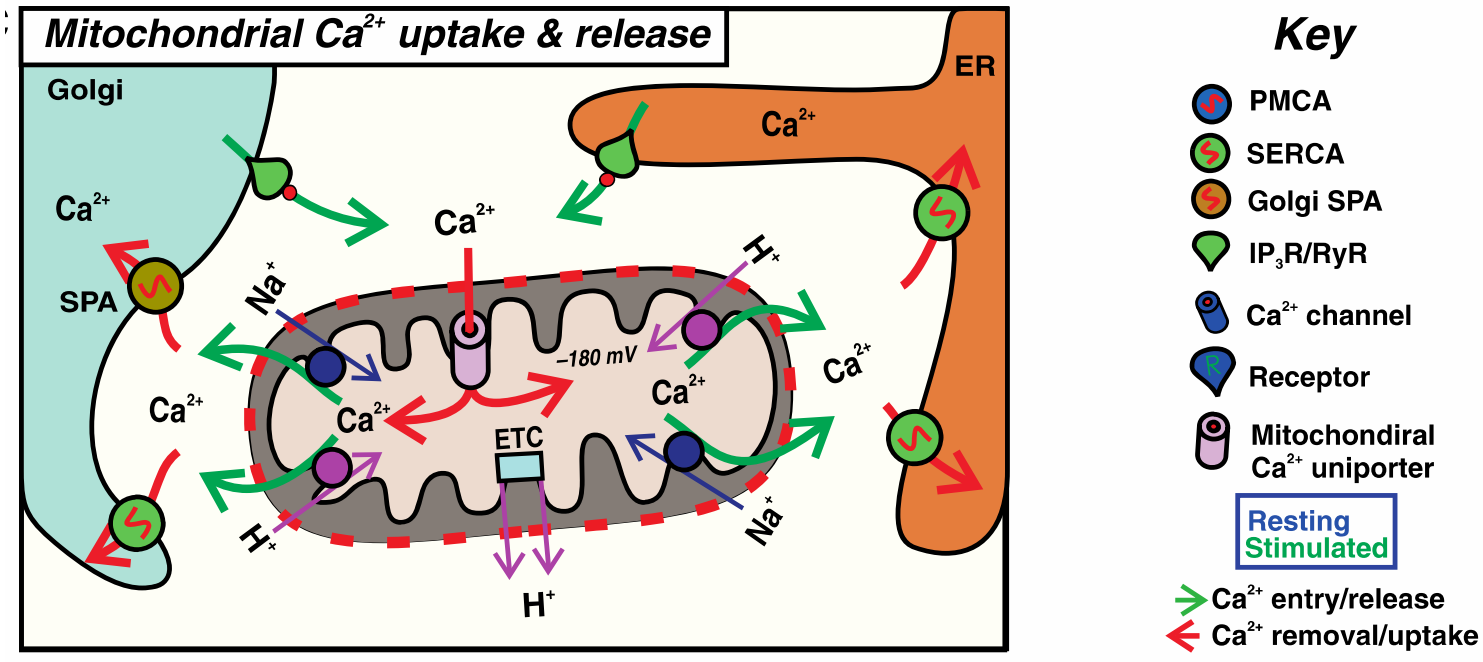

Modified from Alex J. Laude, Alec W. M. Simpson, 2009

↑ $[Ca^{2+}]_m$ ↑ ROS ↑ apoptosis

physical Ca^{2+} compartments: LISOSOMES

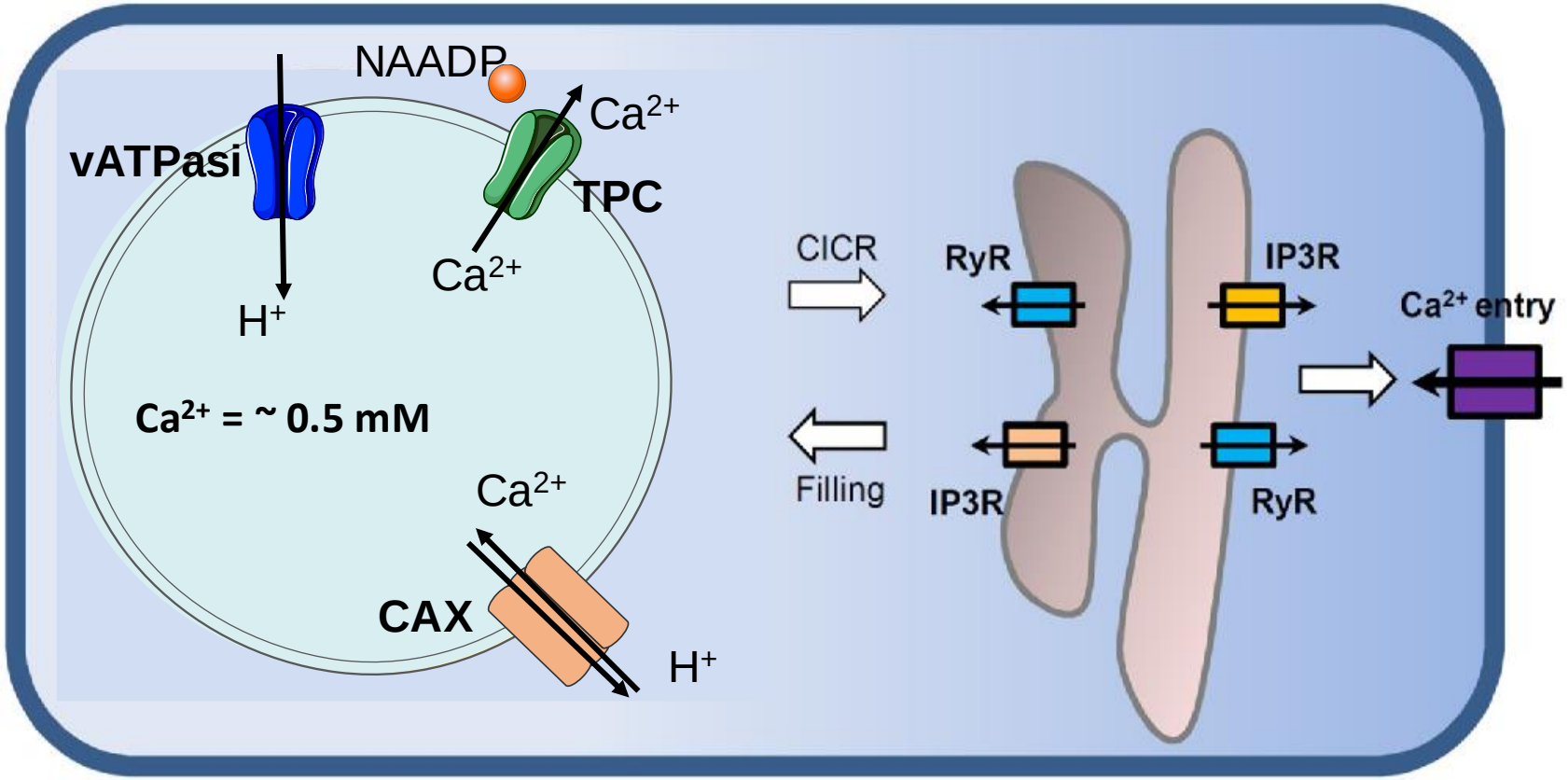

Modified from Xi Zoë Zhong, Yiming Yang, Xue Sun, Xian-ping Dong, Cell Calcium 2017

NAADP: nicotinic acid adenine dinucleotide phosphate
TPC: two pore channel
CAX: Ca^{2+}/H^{+} exchanger

$$NADP \xrightarrow{CD38} NAADP$$

FUNCTIONAL ANALYSES OF ION CHANNELS

Department of
Life Sciences
and Systems Biology

UNIVERSITÀ
DI TORINO

the use of **fluorescent dyes** sensitive to intracellular ions allows functional analysis of the membrane channels

Most studied are molecular probes that specifically binds Ca^{2+} and H^{+}

Ca^{2+} signals by means of fluorescent dyes: how it works

1. fluorescent probe binds intracellular Ca^{2+}
2. it changes its molecular structure
3. and its fluorescence property
4. [Ca^{2+}] can be monitored

FLUORESCENT Ca^{2+} PROBES

Department of
Life Sciences
and Systems Biology

UNIVERSITÀ
DI TORINO

➡ PROTEIC

Genetically Encoded (GECI)

➡ SYNTHETIC

Fluorescent molecules

Probe	Origin	Detection technique
Aequorin	Genetically encoded	Luminometry
Berovin	Genetically encoded	Luminometry
Obelin	Genetically encoded	Luminometry
Cameleon	Genetically encoded	FRET microscopy
Troponin C biosensor	Genetically encoded	FRET microscopy
Camgaroo	Genetically encoded	Fluorescence microscopy
Ratiometric Pericam	Genetically encoded	Ratiometric fluorescence microscopy
GEM-GECO1	Genetically encoded	Ratiometric fluorescence microscopy
Calcium Green-1	Synthetic	Fluorescence microscopy
Fluo-3, Fluo-4	Synthetic	Fluorescence microscopy
Fura-2, Indo-1	Synthetic	Ratiometric fluorescence microscopy

SYNTHETIC fluorescent Ca^{2+} probes

Structurally based on molecular Ca^{2+} chelators: BAPTA or EGTA

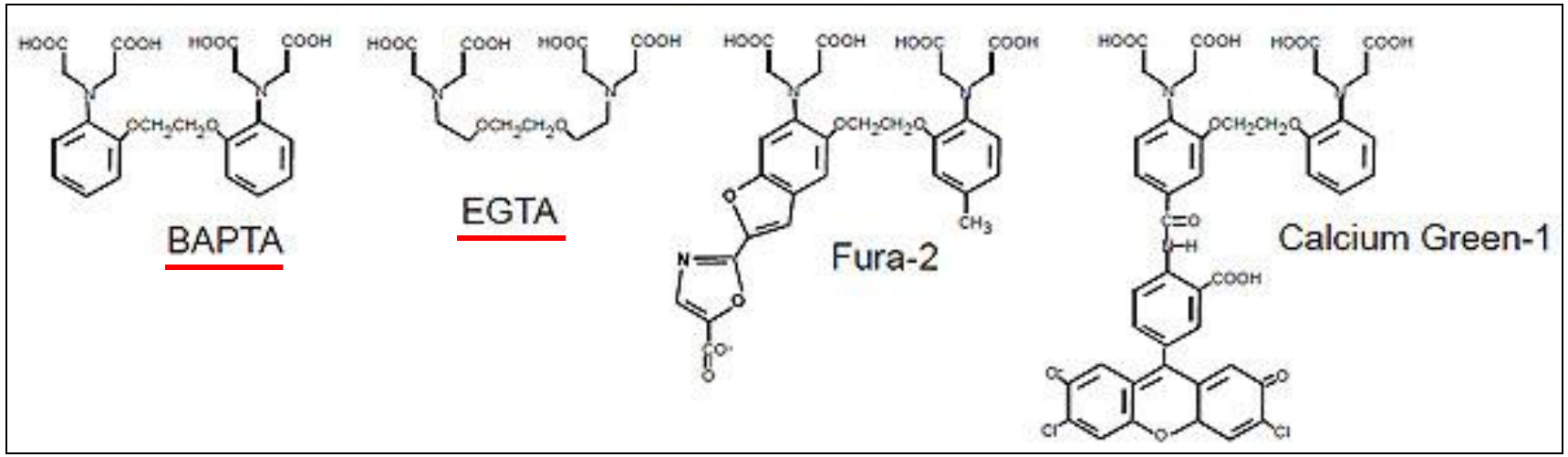

These molecules need to be further implemented in order to express **fluorescence properties**: every Ca^{2+} indicator consists in a fluorescent dye that changes its fluorescent (**ʎ** and **intensity**, emission or excitation) spectrum depending on "Ca^{2+}-bound" or "not bound" state

SYNTHETIC fluorescent Ca^{2+} probes

The dissociation constant (K_d)

$\downarrow K_d$ $\uparrow Ca^{2+}$ affinity

- molar units (M)
- corresponds to the concentration of Ca^{2+} at which half the indicator molecules are bound with Ca^{2+} at equilibrium
- possibly, the indicators should be utilized to measure Ca^{2+} concentrations between 0.1 and 10 times their K_d. This is the range over which Ca^{2+} dependent changes in fluorescence are the largest.

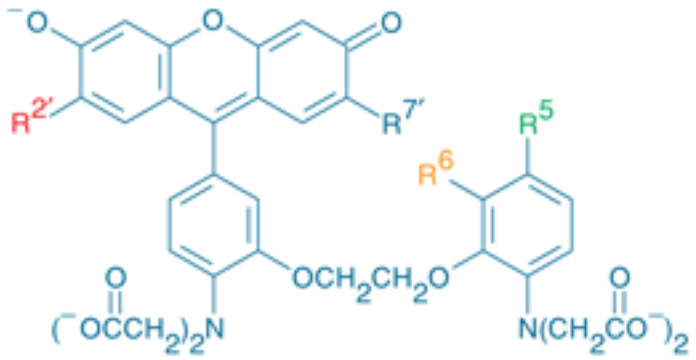

Indicator	$K_d(Ca^{2+})$	$R^{2'}$	$R^{7'}$	R^5	R^6
Fluo-3	0.39 μM	Cl	Cl	CH_3	H
Fluo-4	0.35 μM	F	F	CH_3	H
Fluo-5F	2.3 μM	F	F	F	H
Fluo-5N	90 μM	F	F	NO_2	H
Fluo-4FF	9.7 μM	F	F	F	F

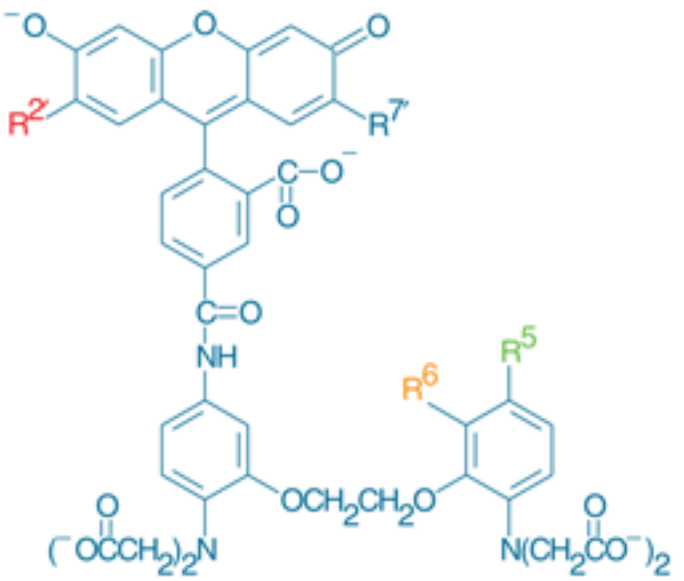

Indicator	$K_d(Ca^{2+})$	$R^{2'}$	$R^{7'}$	R^5	R^6
Calcium Green-1	0.19 μM	Cl	Cl	H	H
Calcium Green-5N	14 μM	Cl	Cl	NO_2	H
Oregon Green 488 BAPTA-1	0.17 μM	F	F	H	H
Oregon Green 488 BAPTA-6F	3 μM	F	F	H	F
Oregon Green 488 BAPTA-5N	20 μM	F	F	NO_2	H

SYNTHETIC fluorescent Ca^{2+} probes

probe incorporation into the cell

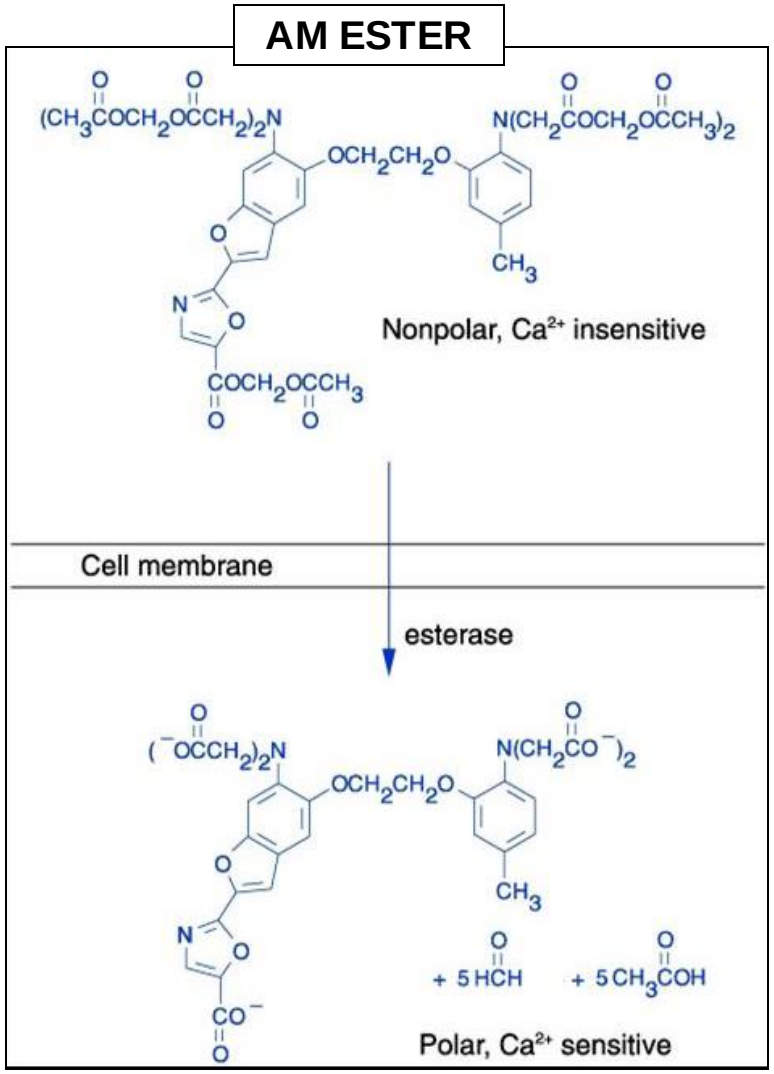

two ways:

1) Microinjection of dextran conjugates or salt form

2) Loading Acetoxymethyl (AM) esters: carboxylic groups of Ca^{2+} indicators are derivatized as acetoxymethyl rendering them permeant to membranes and insensitive to ions.

SYNTHETIC fluorescent Ca^{2+} probes

probe incorporation into the cell

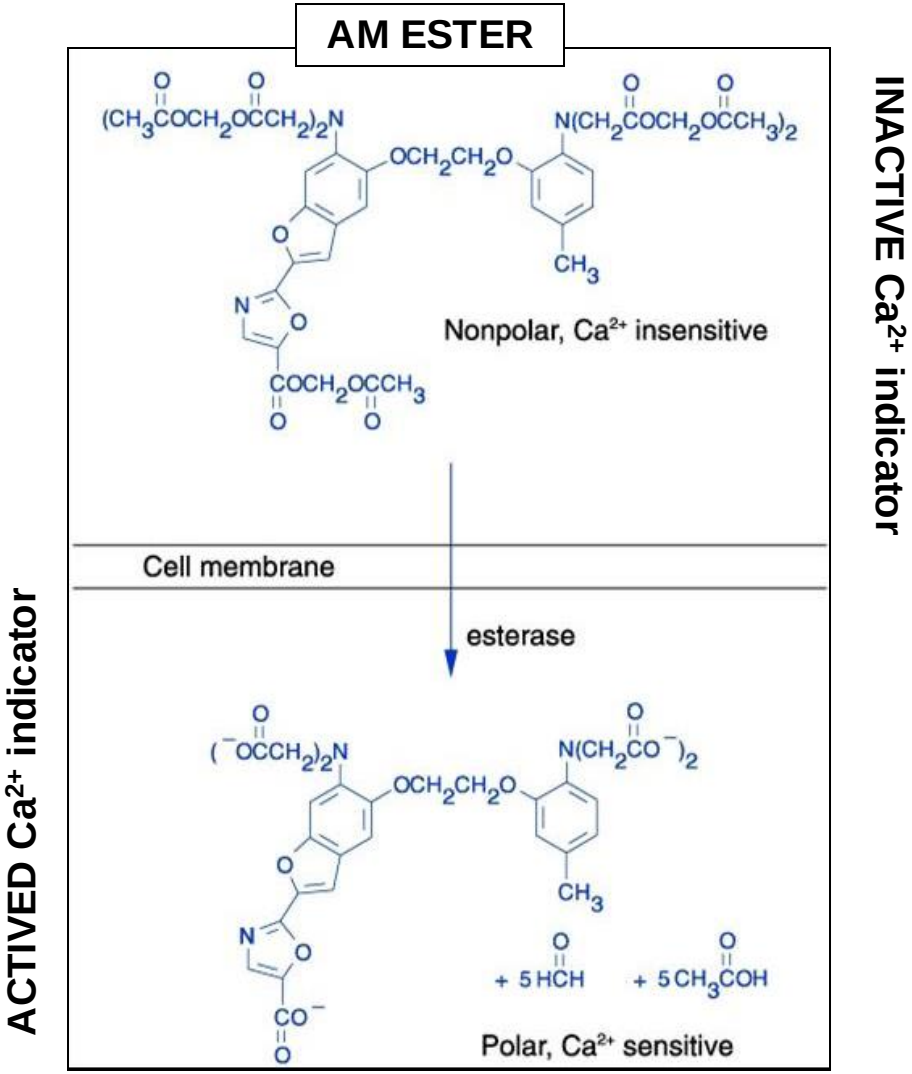

Once inside the cell, these derivatized indicators are hydrolyzed by ubiquitous intracellular esterases and the ion-sensitive indicator is released

SYNTHETIC fluorescent Ca^{2+} probes

Non ratiometric Ca^{2+} indicators

Indicator	K_d (nM)	$\lambda_{excitation}$ (nm)	$\lambda_{emission}$ (nm)
Fluo-3	390	506	526
Fluo-4	345	494	516
Calcium Green-2	550	503	536
Calcium Orange	185	549	575
Fluo-4FF	9700	494	516

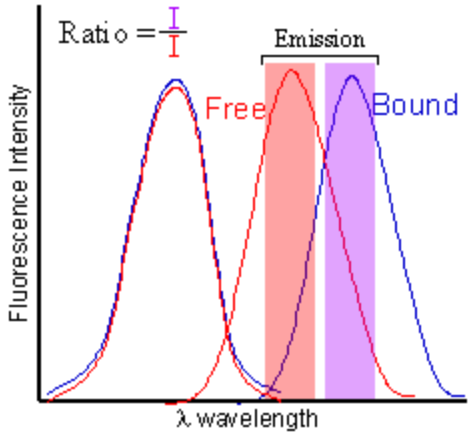

Ratiometric Ca^{2+} indicators

Indicator	K_d (nM)	$\lambda_{excitation}$ (nm)		$\lambda_{emission}$ (nm)	
		Free	Bond	Free	Bond
Fura Red	140	472	436	657	657
Fura-2	145	363	335	512	512
Mag-fura-2	25000	369	329	511	511
Indo-1	230	338	338	475	401

SYNTHETIC fluorescent Ca^{2+} probes

Fluo-3

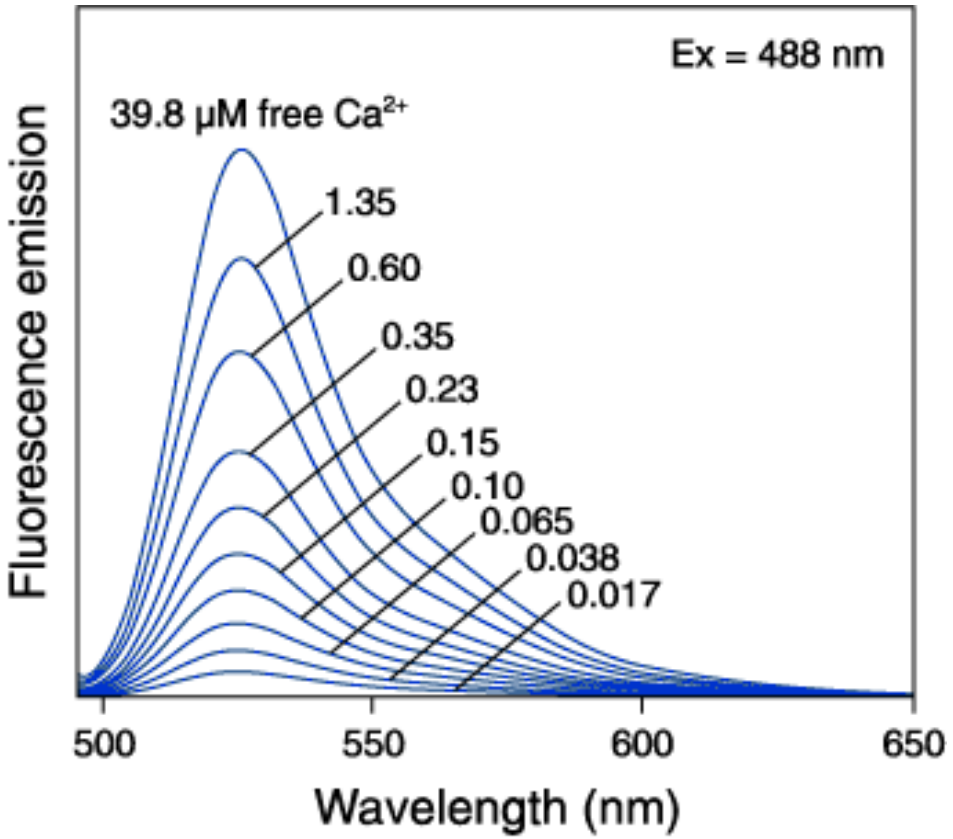

- Excitation at 488 nm (visible light) → Argon laser can be used
- Emission at 525 nm
- K_d (Ca^{2+}) = 0.39 µM
- qualitative detection ✓
- quantitative detection ✗

SYNTHETIC fluorescent Ca^{2+} probes

Fura-2

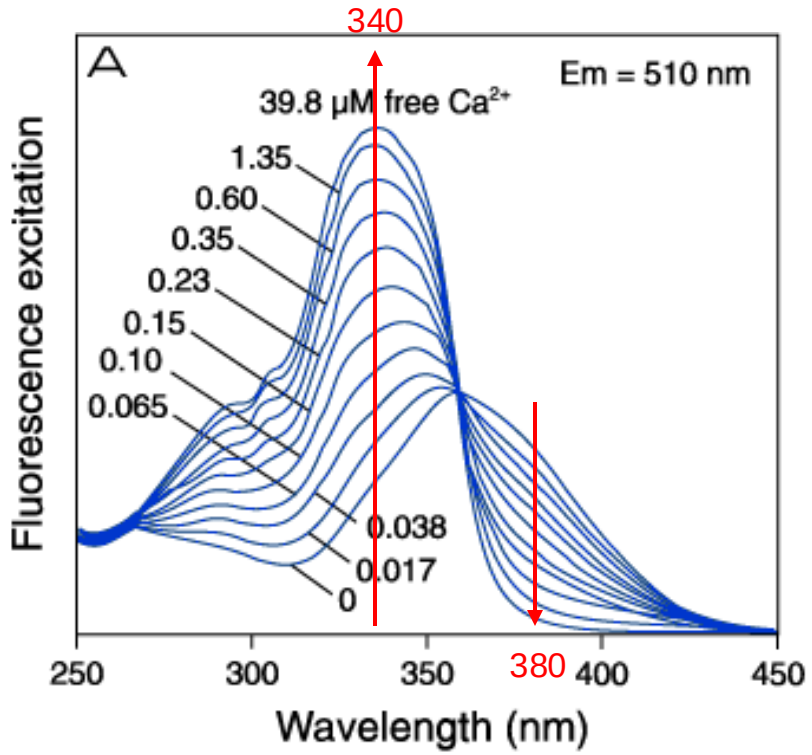

- fixed emission **ratiometric dye**
- excitation at 340 and 380 nm
- emission at 510 nm
- molecular structure derived from BAPTA

- qualitative detection ✓
- quantitative detection ✓

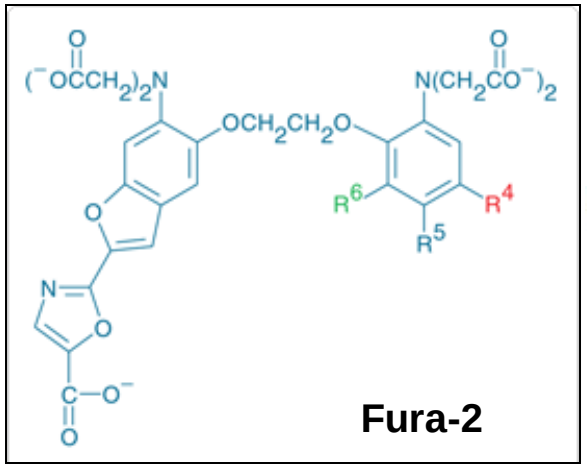

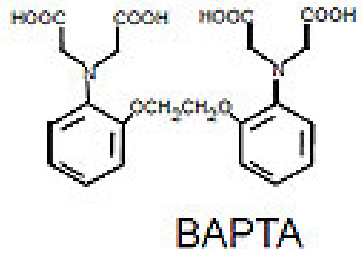

SYNTHETIC fluorescent Ca^{2+} probes

Fura-2

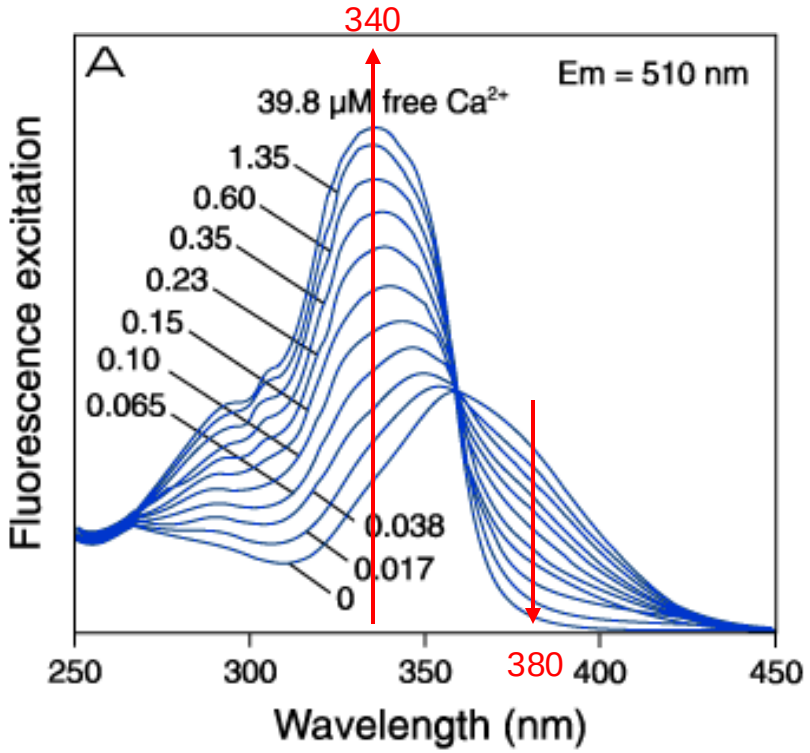

$$R = \frac{I_{em}\,340}{I_{em}\,380}$$

quantitative detection is more precise than single λ indicators because ratio (R) considerably reduces the effects of:

- uneven dye loading
- leakage of dye
- Photobleaching
- cells thickness

SYNTHETIC fluorescent Ca^{2+} probes

Fura-2 (fixed emission ratiometric dye)

Limits:

- limited sensitivity to $[Ca^{2+}] > 1$ µM
- low K_d damped rapid Ca^{2+} transient measurements

$$R = \frac{I_{em}\ 340}{I_{em}\ 380}$$

Molecular Probes offer several Fura-2 derivatives with lower Ca^{2+} binding affinity

Table 1. Spectroscopic properties and Ca^{2+} dissociation constants for fura-2, indo-1, and their derivatives.

Indicator	Catalog Number		Zero Calcium			High Calcium			K_d (Ca^{2+}) (µM)
	Salt	AM Ester	λ_A † (nm)	ϵ_{max} ‡ ($cm^{-1}M^{-1}$)	λ_F § (nm)	λ_A † (nm)	ϵ_{max} ‡ ($cm^{-1}M^{-1}$)	λ_F § (nm)	
fura-2	F1200, F6799	F1201, F1221, F1225, F14185 *	363	28,000	512 **	335	34,000	505 ††	0.14
bis-fura-2	B6810		366	56,000	511	338	68,000	504	0.37
fura-5F	F14176	F14177	363	26,000	512	336	29,000	506	0.40
fura-4F	F14174	F14175	366	21,000	511	336	23,000	505	0.77
fura-6F	F14178	F14179	364	25,000	512	336	28,000	505	5.30
fura-FF	F14180	F14181	364	25,000	510	335	28,000	506	5.50
indo-1	I1202	I1203, I1223, I1226	346	33,000	475 **	330	33,000	401 ††	0.23
indo-5F	I23912	I23913	344	31,000	471	329	31,000	398	0.47

* High-purity FluoroPure™ grade; † absorption maximum; ‡ molar extinction coefficient; § fluorescence emission maximum; ** fluorescence quantum yield 0.23 for fura-2, 0.38 for indo-1. †† Fluorescence quantum yield 0.49 for fura-2, 0.56 for indo-1. Spectroscopic data and K_d (dissociation constant) values measured in 100 mM KCl, 10 mM MOPS, pH 7.20, 0–10 mM CaEGTA at 22°C.

SYNTHETIC fluorescent Ca^{2+} probes

Department of
Life Sciences
and Systems Biology

Measurements and Calibration for Fura Indicators

The absorption (or fluorescence excitation) maximum of Fura indicators shifts from **363nm** for the Ca^{2+}- free chelator (Zero Calcium) to about **335nm** for the Ca^{2+}-bound (High Calcium). The wavelength of maximum fluorescence emission is relatively independent of Ca^{2+} concentration.

Table 1. Spectroscopic properties and Ca^{2+} dissociation constants for fura-2, indo-1, and their derivatives.

Indicator	Catalog Number		Zero Calcium			High Calcium			K_d (Ca^{2+}) (μM)
	Salt	AM Ester	λ_A † (nm)	ϵ_{max} ‡ ($cm^{-1}M^{-1}$)	λ_F § (nm)	λ_A † (nm)	ϵ_{max} ‡ ($cm^{-1}M^{-1}$)	λ_F § (nm)	
fura-2	F1200, F6799	F1201, F1221, F1225, F14185 *	363	28,000	512 **	335	34,000	505 ††	0.14
bis-fura-2	B6810		366	56,000	511	338	68,000	504	0.37
fura-5F	F14176	F14177	363	26,000	512	336	29,000	506	0.40
fura-4F	F14174	F14175	366	21,000	511	336	23,000	505	0.77
fura-6F	F14178	F14179	364	25,000	512	336	28,000	505	5.30
fura-FF	F14180	F14181	364	25,000	510	335	28,000	506	5.50
indo-1	I1202	I1203, I1223, I1226	346	33,000	475 **	330	33,000	401 ††	0.23
indo-5F	I23912	I23913	344	31,000	471	329	31,000	398	0.47

* High-purity FluoroPure™ grade; † absorption maximum; ‡ molar extinction coefficient; § fluorescence emission maximum; ** fluorescence quantum yield 0.23 for fura-2, 0.38 for indo-1. †† Fluorescence quantum yield 0.49 for fura-2, 0.56 for indo-1. Spectroscopic data and K_d (dissociation constant) values measured in 100 mM KCl, 10 mM MOPS, pH 7.20, 0–10 mM CaEGTA at 22°C.

SYNTHETIC fluorescent Ca^{2+} probes

Department of
Life Sciences
and Systems Biology

UNIVERSITÀ DI TORINO

Measurements and Calibration for Fura Indicators

$$R = \frac{I_{em}\,340}{I_{em}\,380}$$

The largest dynamic range for Ca^{2+}-dependent fluorescence signals is obtained by using excitation at 340 nm and 380 nm and ratioing the fluorescence intensities detected at 510 nm.

Intracellular [Ca^{2+}] can be estimated using dissociation constants (K_d) that are derived from **calibration curves**

Calibrating Fura indicators:

1) to determine Kd: measurements for the completely ion-free and ion-saturated indicator (to determine the values for **F_{min}, F_{max}, R_{min}, and R_{max}**) and for the indicator in the presence of known Ca^{2+} concentrations
2) Once the indicator has been calibrated with solutions of known [Ca^{2+}], the following equation can be used to relate the intensity ratios to Ca^{2+} levels

$$[Ca^{2+}] = K_d\, Q \frac{(R - R_{min})}{(R_{max} - R)}$$

SYNTHETIC fluorescent Ca^{2+} probes

Measurements and Calibration for Fura Indicators

$$[Ca^{2+}] = K_d \, Q \frac{(R - R_{min})}{(R_{max} - R)}$$

Kd is *the dissociation constant*

Q is *the* ***ratio of Fmin to Fmax at λ2*** (~380 nm)

R represents the ***fluorescence intensity ratio Fλ1/Fλ2***

λ1 (~340 nm) fluorescence detection for the ion-bound indicator

λ2 (~380 nm) fluorescence for the ion-free indicator

Ratios corresponding to the titration end points are denoted by the subscripts indicating the minimum and maximum Ca^{2+} concentration (from the calibration curve)

SYNTHETIC fluorescent Ca^{2+} probes

Indo-1

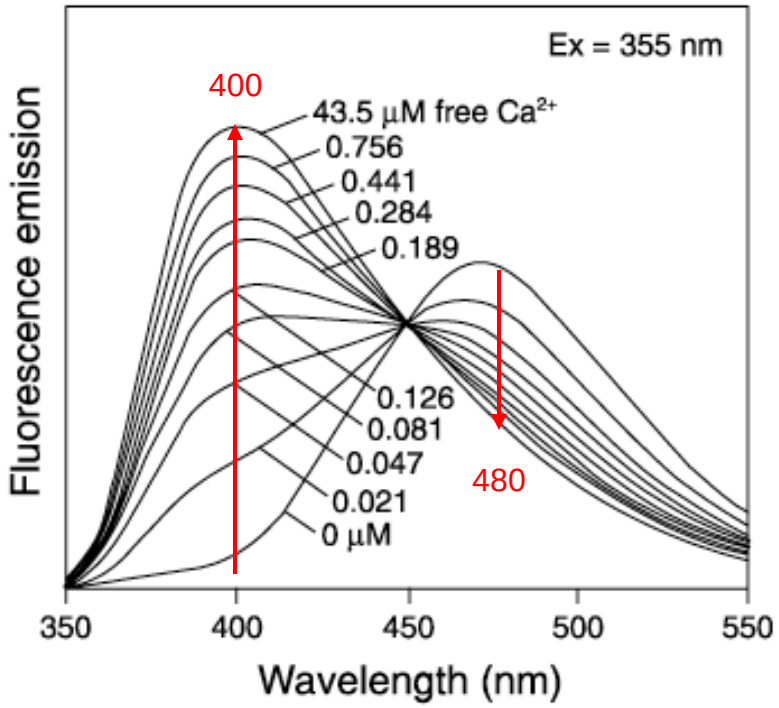

- fixed excitation **ratiometric dye**
- excitation at 335 nm
- emission at 400 and 480 nm

Free Ca^{2+} Concentration in a Purkinje Neuron from Embryonic Mouse Cerebellum

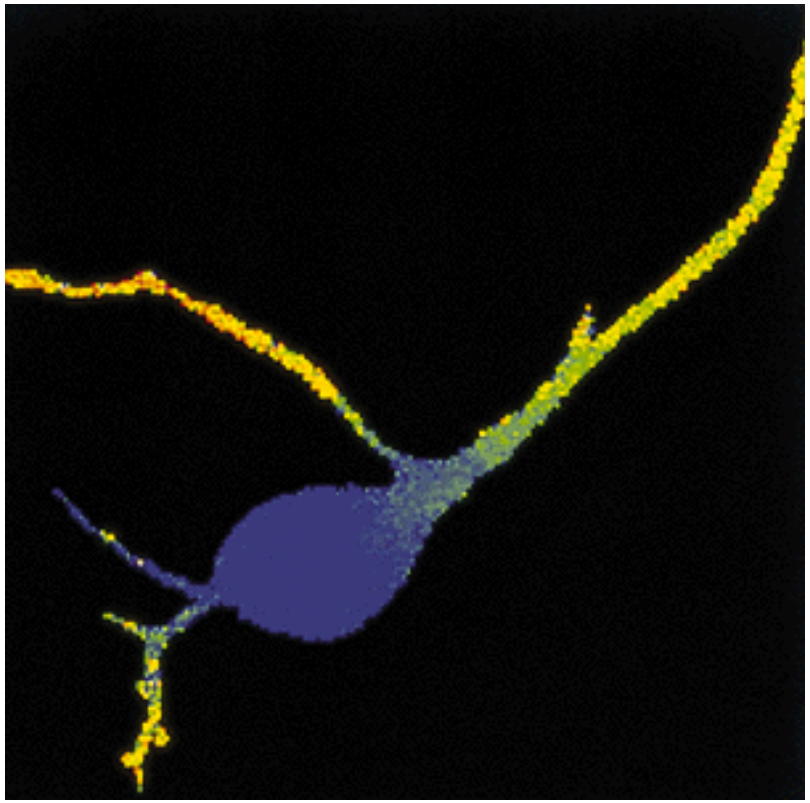

- Neurons were loaded with Fura-2.
- Neurons were stimulated with glutamate receptor agonist.
- The composite image represents the ratio of images obtained with excitation at 340 nm and 380 nm.

SYNTHETIC fluorescent Ca^{2+} probes

Dual Blu Ca^{2+} INDICATORS:

Fluo-3 and **Fura Red**

- Use of two dyes solves the problem:

e.g. **Fluo-3** (increase at 525 with increasing [Ca^{2+}]) and **Fura Red** (decrease at 650 upon increasing [Ca^{2+}]).

- Both excited by 488 nm

- Indipendent from [dye]

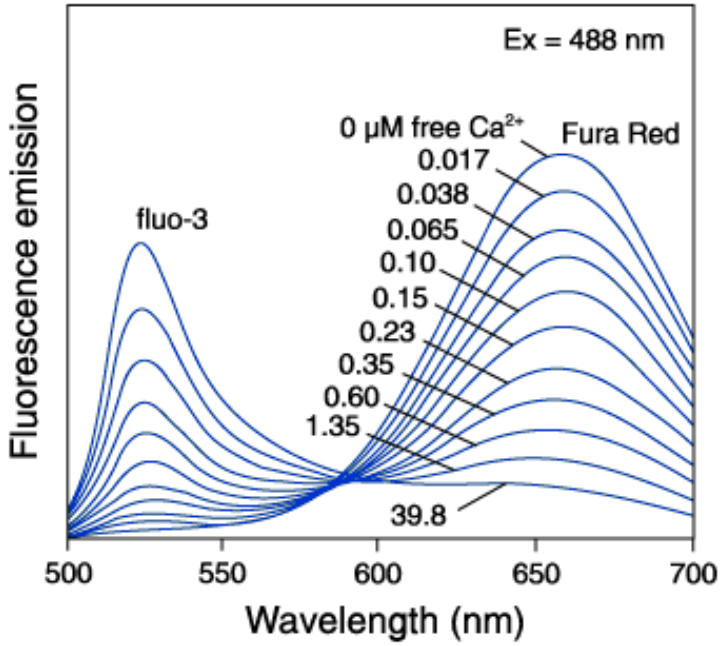

$$[Ca^{2+}] = \frac{I_{em}\,Fluo3}{I_{em}\,Fura\,Red} \quad \begin{matrix}(525\text{ nm})\\(650\text{ nm})\end{matrix}$$

PROTEIC fluorescent Ca^{2+} probes

GCaMP

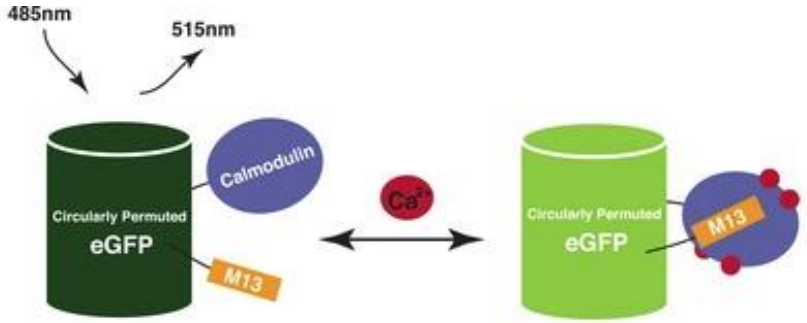

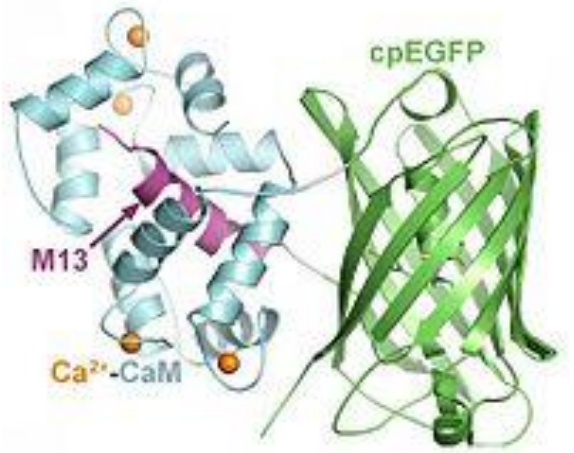

The sensor comprises a circularly permuted **eGFP** (cqGFP) flanked by **CaM** and a CaM-binding peptide (**M13**) from myosin light chain kinase.
Increases in Ca^{2+} promote **Ca^{2+}-CaM-M13** interaction and a conformational change within the sensor → thus results in increased eGFP fluorescence

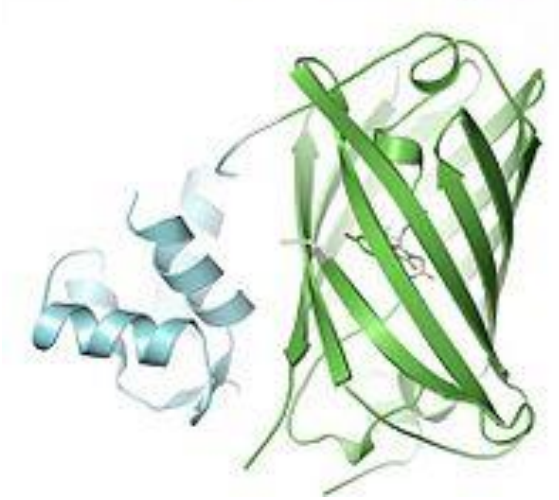

Willoughby, D. et al. J Cell Sci 2010;123:107-117

nature COMMUNICATIONS

ARTICLE

Received 16 Jan 2014 | Accepted 16 May 2014 | Published 13 Jun 2014

DOI: 10.1038/ncomms5153 OPEN

Imaging intraorganellar Ca^{2+} at subcellular resolution using CEPIA

Junji Suzuki[1], Kazunori Kanemaru[1], Kuniaki Ishii[2], Masamichi Ohkura[3], Yohei Okubo[1] & Masamitsu Iino[1]

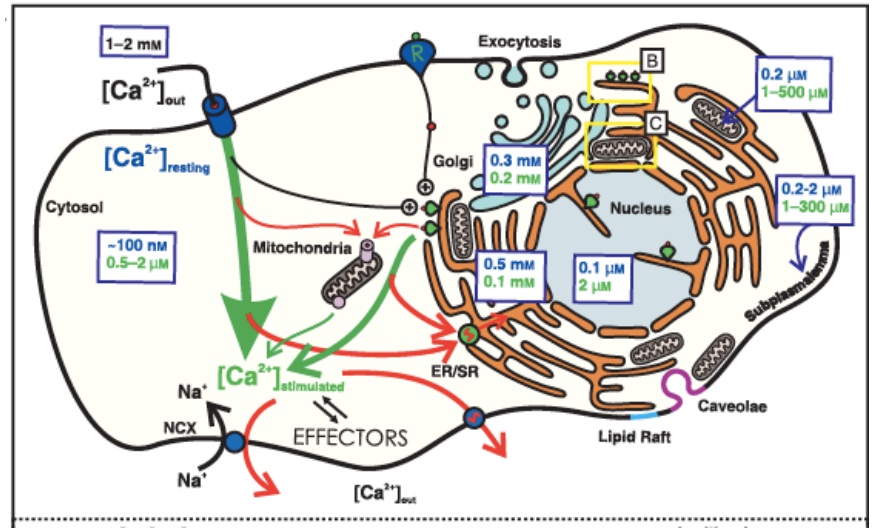

Both ER and mitochondrial membranes display Ca2+-transporting molecules whose function is to import Ca2+ into the lumen against the concentration gradient. This uphill Ca2+ transport is mediated in the ER membrane by sarco(endo)plasmic reticulum Ca2+ ATPase (SERCA) and in the inner mitochondrial membrane by the mitochondrial Ca2+ uniporter (MCU).

The organellar membranes also feature molecules that allow Ca2+ to exit from the organelles to the cytosol: inositol 1,4,5-trisphosphate receptors and ryanodine receptors in the ER, and the Na+/Ca2+ and H+/Ca2+ exchangers in mitochondria.

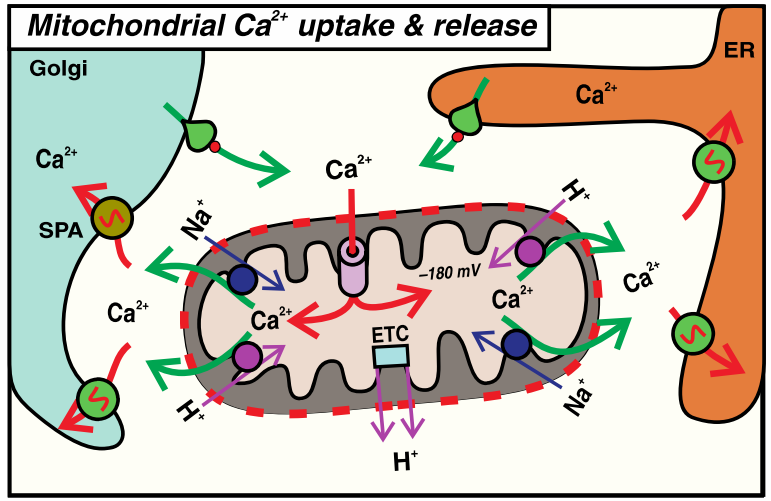

Modified from Alex J. Laude, Alec W. M. Simpson, 2009

Backbone of cfGCaMP2

Kd = 0.67 uM

- Since ER Ca2+ concentration ([Ca2+]ER) is assumed to reach the sub-millimolar range, cfGCaMP2 was engineered to reduce its Ca2+ binding affinity by a factor of ~ 1,000.

variants that were generated in our search we selected one with E31D/F92W/E104D/D133E substitutions that had a low Ca2+ affinity (Kd = 368 uM) and a large dynamic range (Fmax/Fmin = 4.2)

- ER localization and retention signal sequences

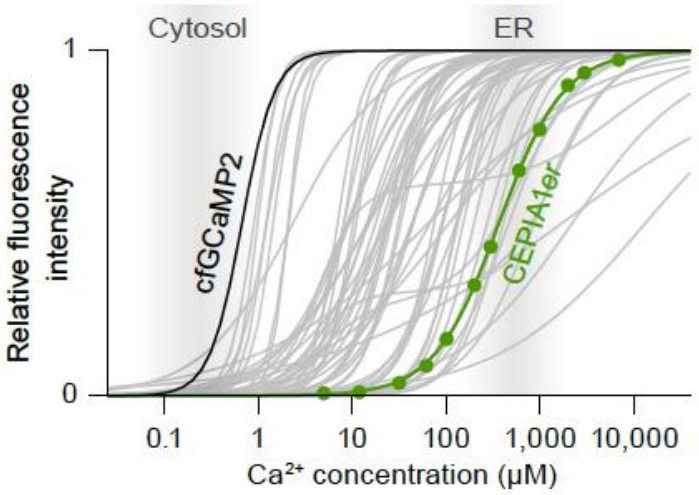

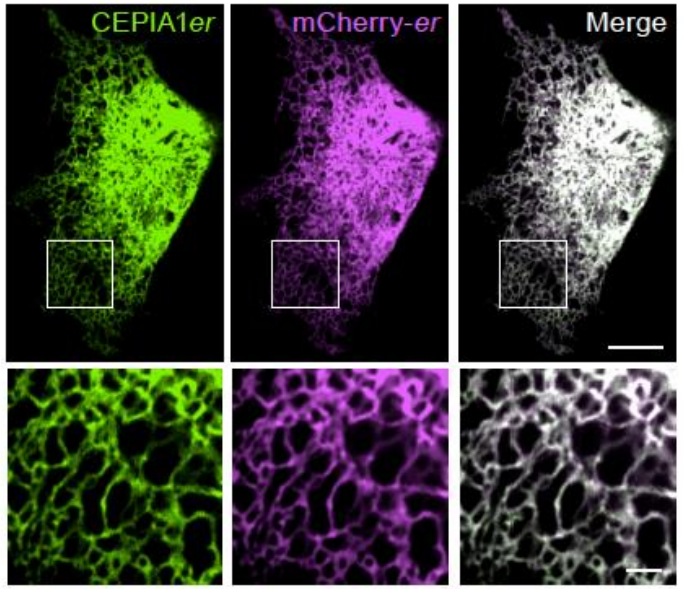

Calcium-measuring organelle-Entrapped Protein IndicAtor 1 in the ER (**CEPIA1er**).

Different colour variants:

R-CEPIA1er (Kd = 565 uM, Fmax/Fmin = 8.8),

G-CEPIA1er (Kd = 672 uM, Fmax/Fmin = 4.7)

GEM-CEPIA1er (Kd = 558 uM, Rmax/Rmin = 21.7) ratiometric dual color

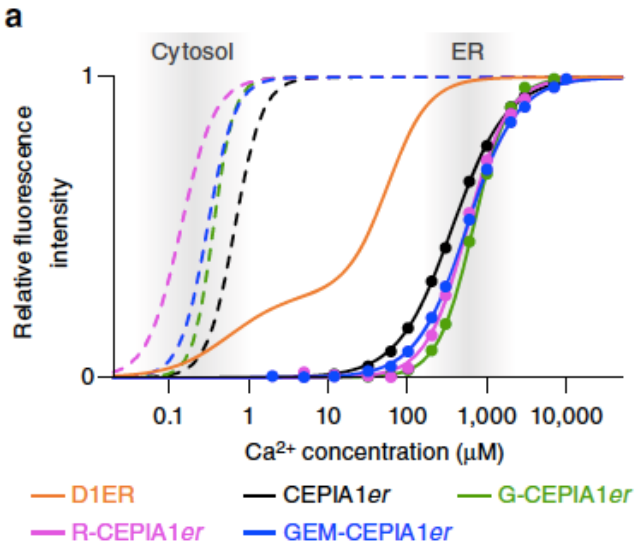

Table 1 | Properties of CEPIA variants.

Probe	Ca^{2+}	ε ($mM^{-1}cm^{-1}$) (λ_{ABS}*)	λ_{Ex}*	Φ (λ_{Em}*)	Brightness† ($mM^{-1}cm^{-1}$)	pK_a‡	Dynamic range§	K_d for Ca^{2+}	Hill coefficient
G-CEPIA1*er*	−	36 (402), 3 (498)	499	0.19 (512)	0.5	8.7	4.7 ± 0.3‖	672 ± 23 μM‖	1.95 ± 0.07‖
	+	33 (401), 10 (497)	498	0.40 (511)	3.4	8.0			
G-GECO1.1	−	35 (401), 2 (500)	499	0.20 (514)	0.4	8.8	14.7 ± 1.6	363 ± 4 nM	3.38 ± 0.10
	+	24 (397), 26 (497)	498	0.46 (513)	10.5	7.4			
R-CEPIA1*er*	−	25 (445), 5 (576)	570	0.09 (593)	0.5	8.9	8.8 ± 0.7	565 ± 58 μM	1.70 ± 0.04
	+	15 (448), 35 (562)	561	0.18 (584)	6.2	6.5, 9.0			
R-GECO1	−	27 (445), 7 (576)	565	0.06 (594)	0.4	8.9	15.6 ± 4.1	142 ± 17 nM	2.05 ± 0.12
	+	58 (562)	560	0.20 (584)	11.6	6.4			
GEM-CEPIA1*er*	−	36 (401)	381, 395	0.26 (510)	9.4	6.1	21.7 ± 0.6	558 ± 14 μM	1.37 ± 0.01
	+	36 (391)	381, 394	0.21 (462)|	7.6	6.5, 10.6			
GEM-GECO1	−	34 (395)	387, 395	0.31 (510)	10.7	6.1	67.5 ± 10.9	306 ± 0.4 nM	2.55 ± 0.02
	+	35 (391)	387, 390	0.18 (462)	6.2	6.1, 10.1			

*λ_{ABS}, λ_{Ex} and λ_{Em} are the maximum wavelength of absorption, fluorescence excitation and fluorescence emission spectra, respectively.
†Brightness is the product of molar extinction coefficient (ε) and quantum yield (Φ).
‡pKa is determined as the pH at half-maximal fluorescence intensity calculated by fitting Hill equation to each plot. As for R-CEPIA1er, GEM-GECO1 and GEM-CEPIA1er, pKa is calculated by double Hill equation (See Methods).
§Dynamic range indicates the ratio of the maximum to minimum fluorescence intensity (F_{max}/F_{min}) or fluorescence ratio (R_{max}/R_{min}) (See Methods).
‖Mean ± s.e.m.

FUNCTIONAL VALIDATION

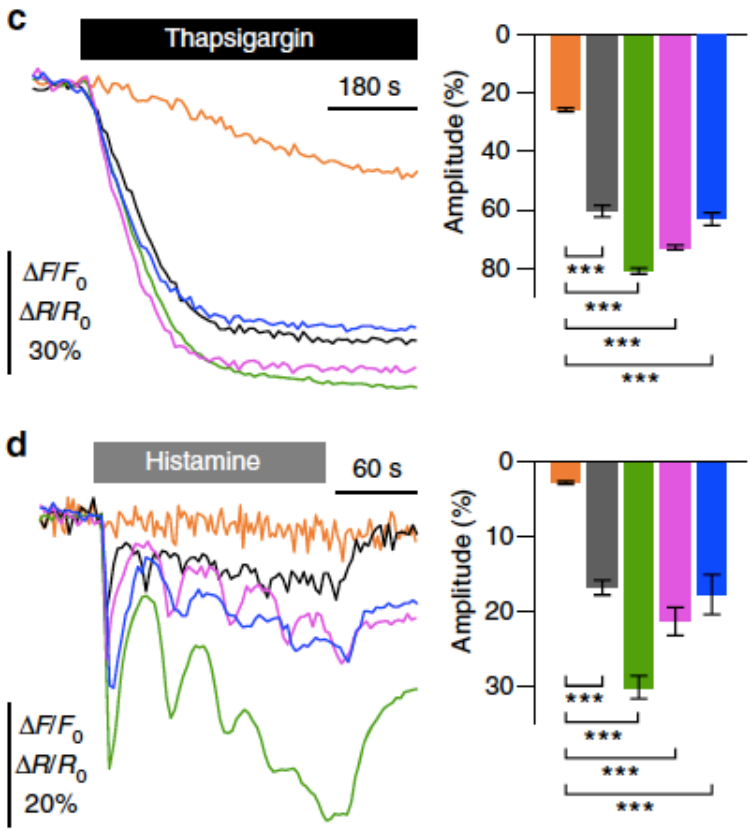

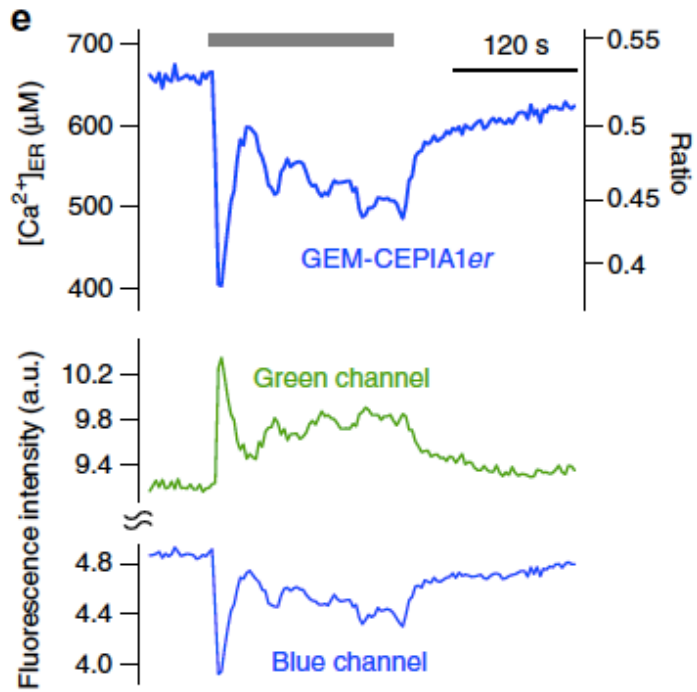

Simultaneous imaging of Ca2+ dynamics in the ER and cytosol

Ca2+ Oscillations induced by Histamine

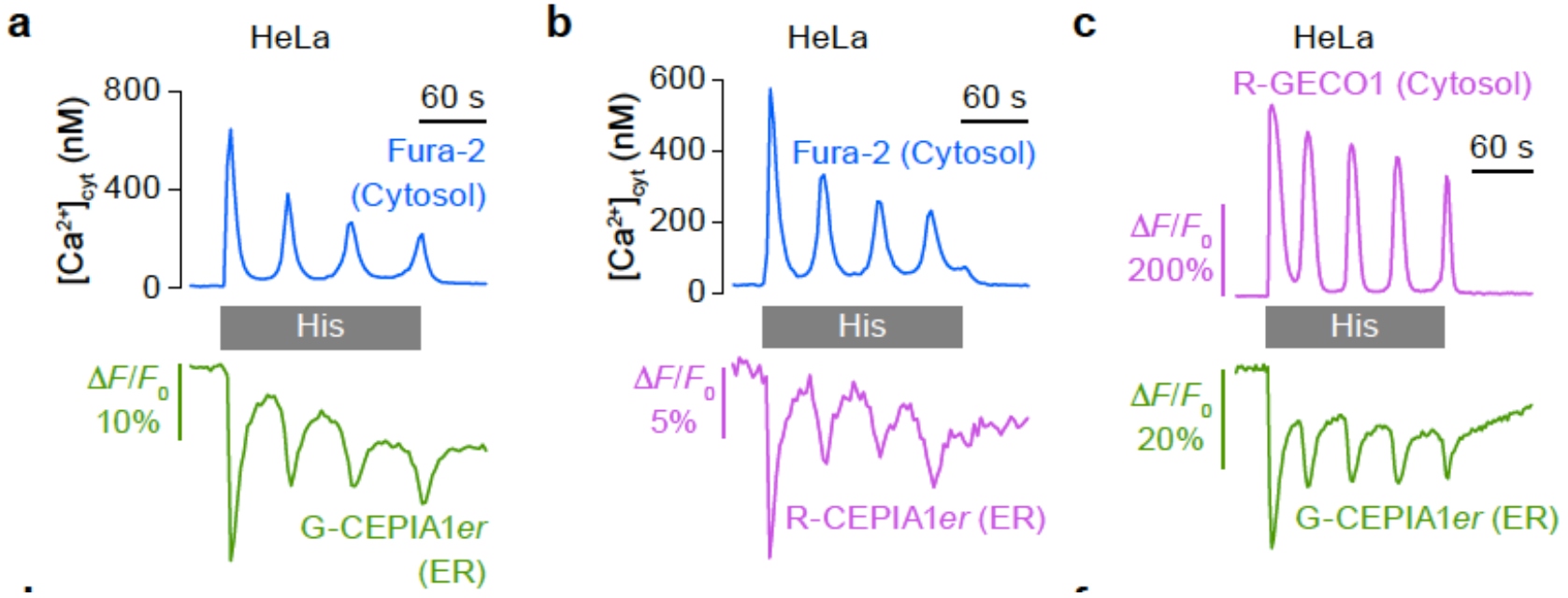

Simultaneous imaging of Ca2+ dynamics in the ER and cytosol

SOCE

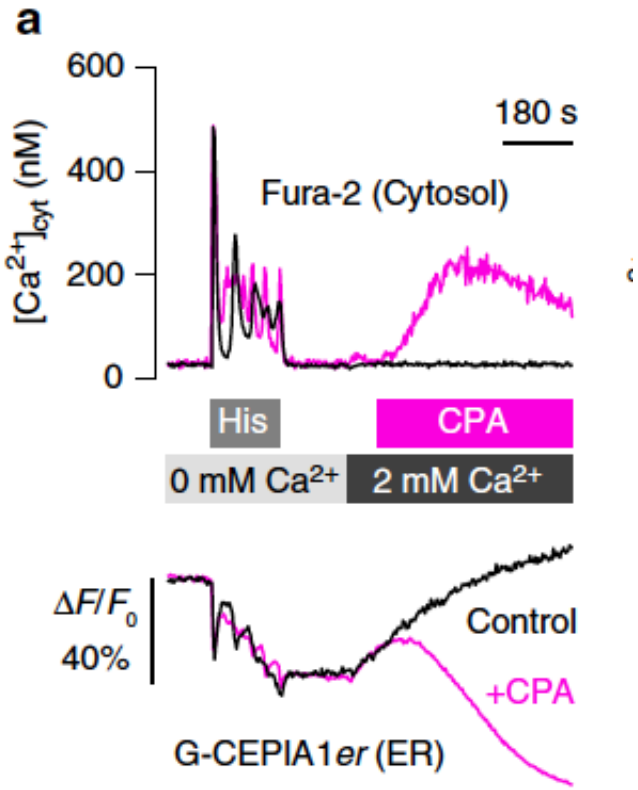

Mitochondrial Ca2+ probe = CEPIA mt

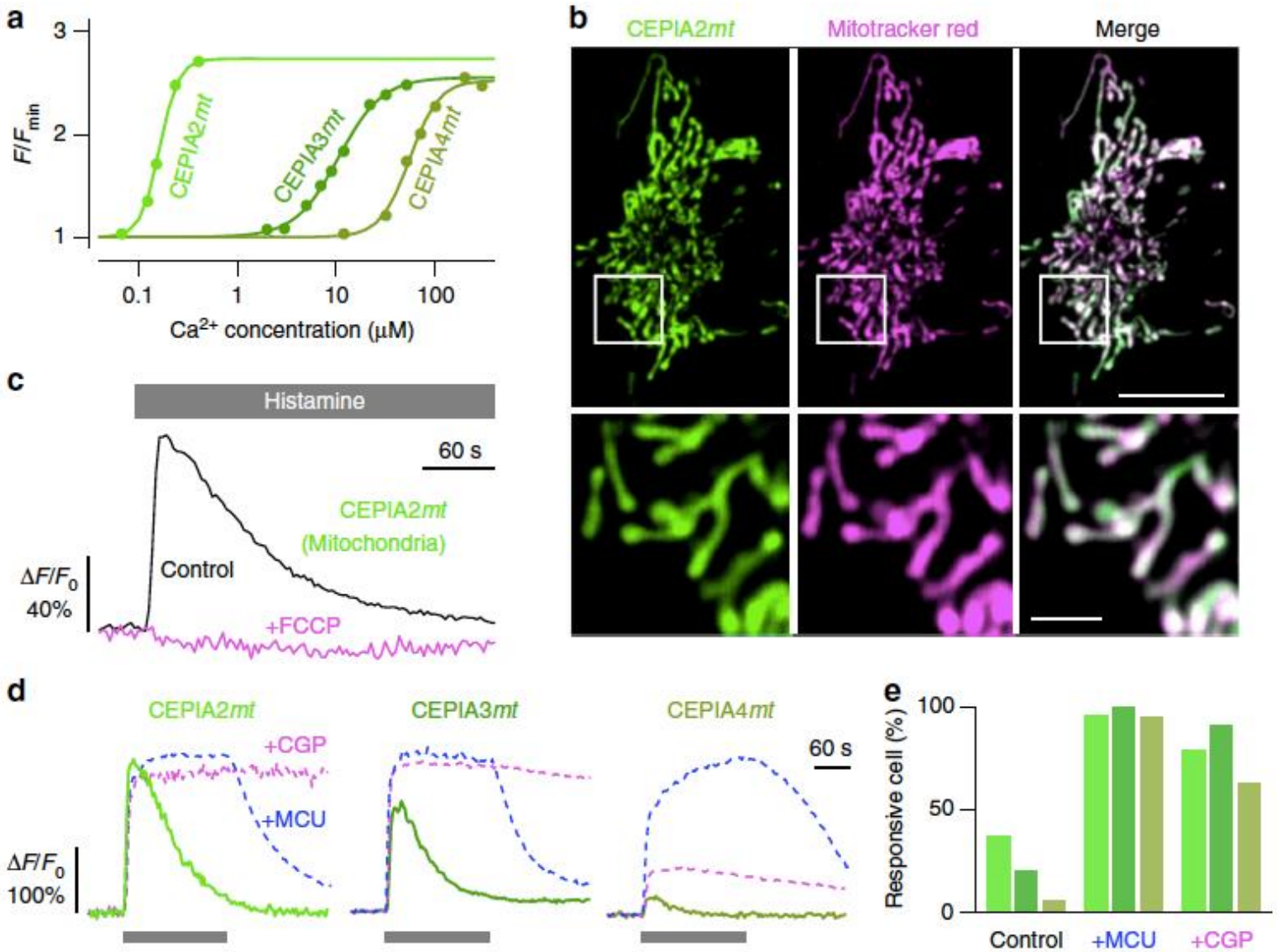

Simultaneous Ca2+ measurements Cytosol – ER-Mt

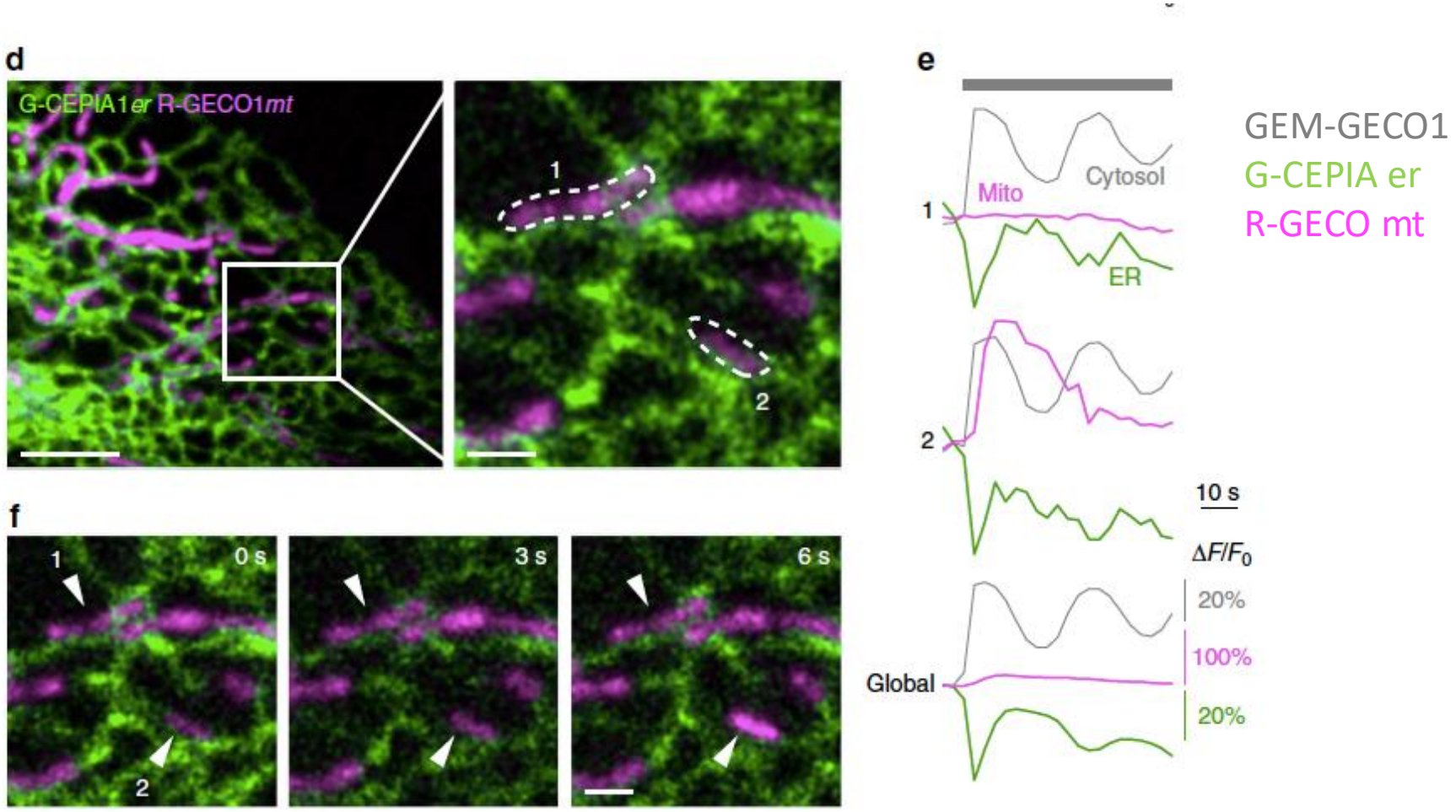

GEM-GECO1
G-CEPIA er
R-GECO mt

SYNTHETIC or PROTEIC fluorescent Ca^{2+} probes

Pros and Cons

None of these protein-based indicators have yet surpassed the sensitivity and speed of commonly used synthetic Ca^{2+} indicators (for example, Oregon Green Bapta-1-AM, OGB1-AM).

Therefore, depending on the experimental goals, investigators choose between sensitive synthetic indicators delivered by invasive chemical or physical methods, or less sensitive protein sensors delivered by genetic methods.

This is of particular interest mainly in neurons.

Because neurons have unusually fast Ca^{2+} dynamics and low peak Ca^{2+} accumulations, sensors designed to probe neuronal function are best tested in neurons rather than in non-neuronal systems, most of which show much slower and larger calcium changes.

Make sense therefore to screen **GCaMP variants,** produced by mutagenesis in neurons and subsequently validated lead sensors, in several *in vivo* systems

… despite extensive structure-guided optimization GCaMP and other protein sensors still suffer from low sensitivity and slow kinetics

Ultrasensitive fluorescent proteins for imaging neuronal activity

Tsai-Wen Chen[1], Trevor J. Wardill[1]†, Yi Sun[1], Stefan R. Pulver[1], Sabine L. Renninger[2], Amy Baohan[1,3], Eric R. Schreiter[1], Rex A. Kerr[1], Michael B. Orger[2], Vivek Jayaraman[1], Loren L. Looger[1], Karel Svoboda[1] & Douglas S. Kim[1]

18 JULY 2013 | VOL 499 | NATURE | 295

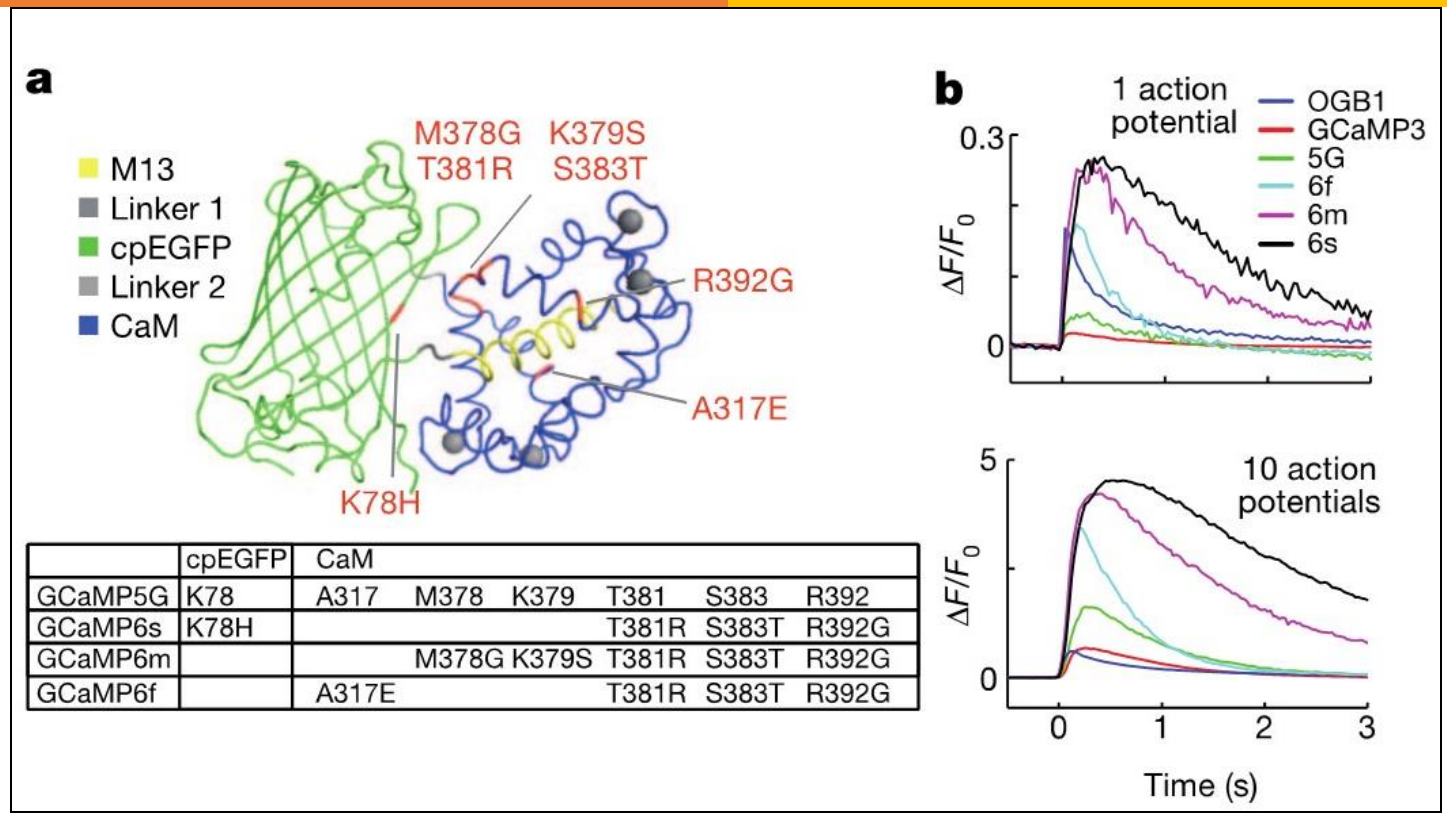

	cpEGFP	CaM					
GCaMP5G	K78	A317	M378	K379	T381	S383	R392
GCaMP6s	K78H				T381R	S383T	R392G
GCaMP6m			M378G	K379S	T381R	S383T	R392G
GCaMP6f		A317E			T381R	S383T	R392G

We produced numerous additional GCaMP variants and tested them in automated neuronal assays (Fig. 1). With the aim of improving sensitivity, we focused mutagenesis on the interface between cpGFP and CaM at 16 amino acid positions, some mutagenized to near completion (Fig. 1a).
Mutations were made at 18 additional sites, notably at the M13–CaM interface which can affect calcium affinity (A317) and in CaM (R392) (Fig. 1a).

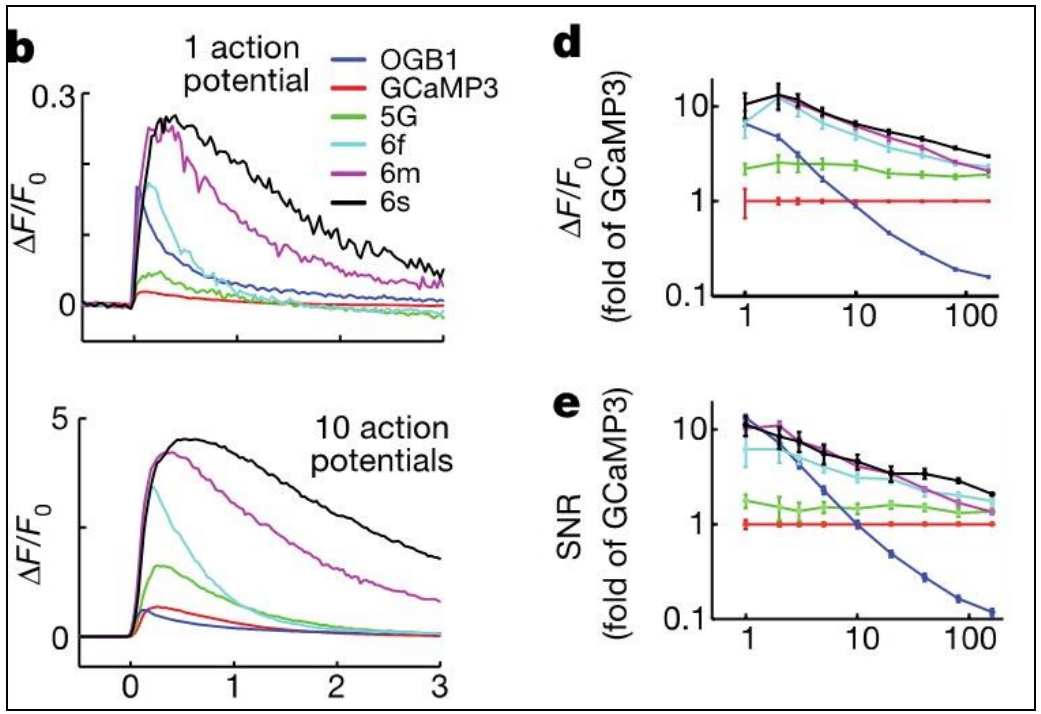

Dissociated rat hippocampal neurons in 24-well plates were transduced with GCaMP variants (one per well), together with nuclear mCherry, using lentivirus-mediated gene transfer. Electrodes triggered trains of action potentials in all neurons within each well.

Time-lapse images (35Hz) of 800 mm fields of view containing 10–100 neurons were acquired, while delivering a series of action potential trains (Fig. 1b).

Fluorescence changes extracted from single neurons were used to compare the sensitivity, dynamic range and kinetics of individual GCaMP variants and OGB1-AM (Fig. 1b–g). We monitored the resting brightness of the sensor by measuring green fluorescence relative to red mCherry fluorescence.

In total, we screened 447 GCaMP variants (Supplementary Table 5).
Based on screening in cultured neurons (Fig. 1), **we chose three ultrasensitive GCaMP6 sensors (GCaMP6s, 6m, 6f; for slow, medium and fast kinetics, respectively) for characterization in vivo.**

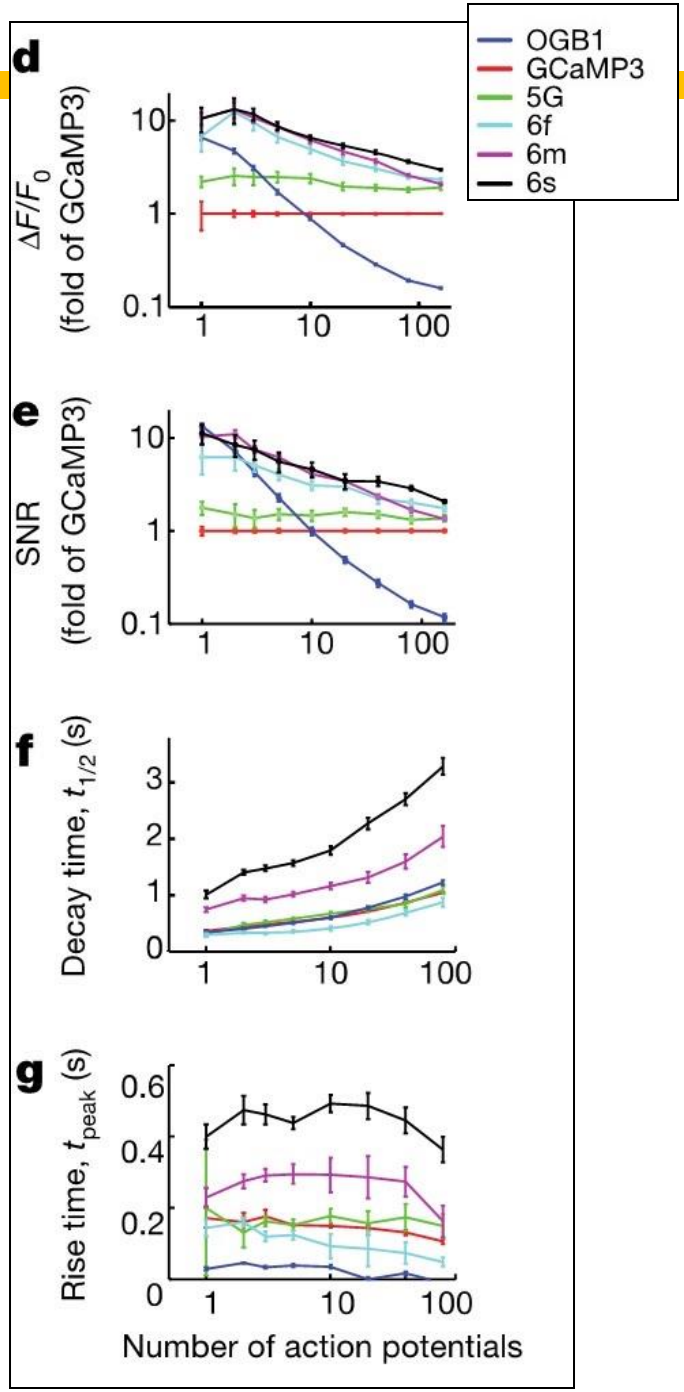

For small numbers of action potentials the most sensitive sensor, GCaMP6s, produced sevenfold larger signals (10-fold larger than GCaMP3, Fig. 1b–e). The fastest sensor, **GCaMP6f**, had two fold faster rise time and 1.7-fold faster decay time than GCaMP5G (Fig. 1f, g). **GCaMP6f is the fastest genetically-encoded calcium indicator for cytoplasmic free calcium in neurons, with sensitivity comparable to OGB1-AM**(Fig. 1d–g).

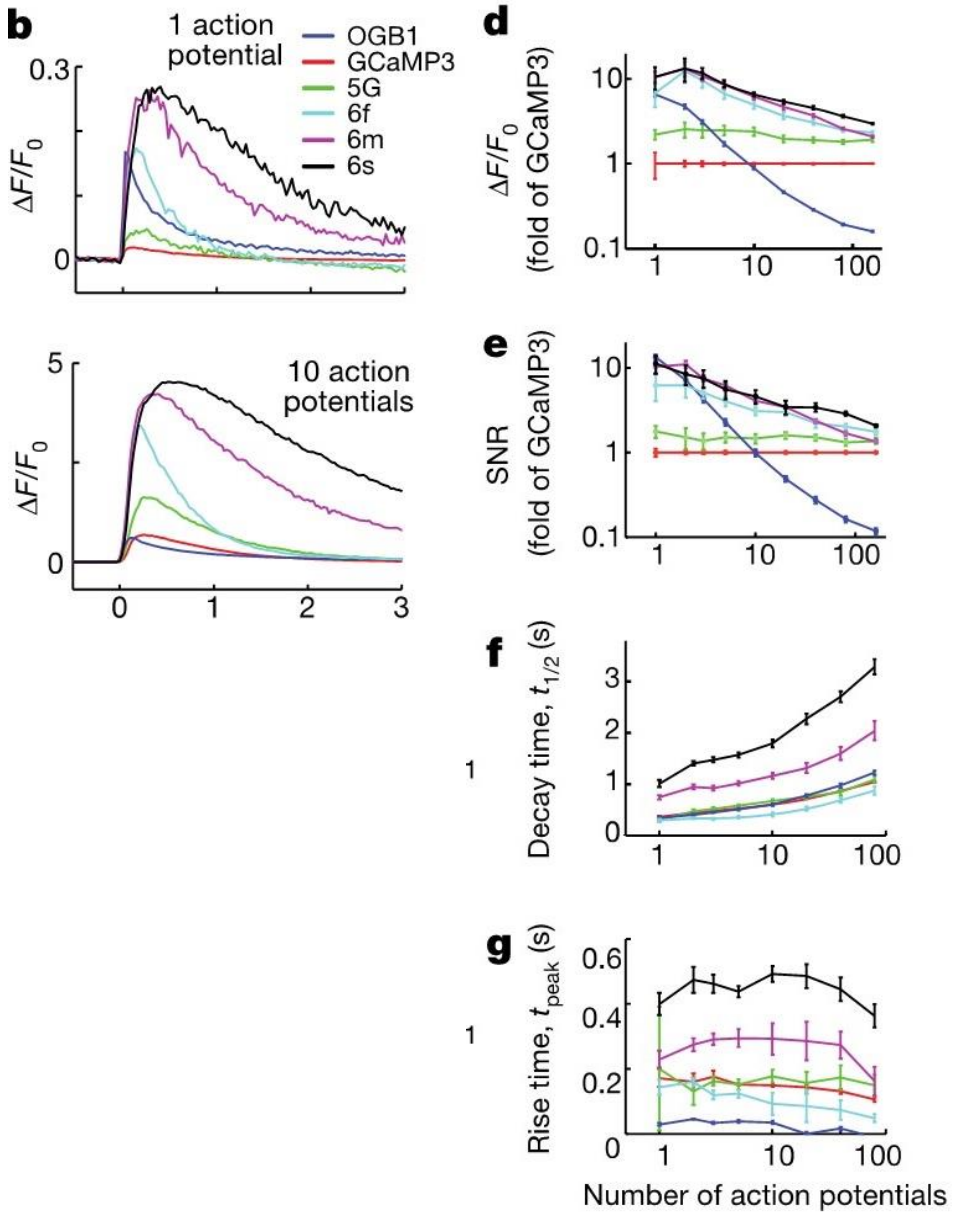

GCaMP6 performance in the mouse visual cortex.

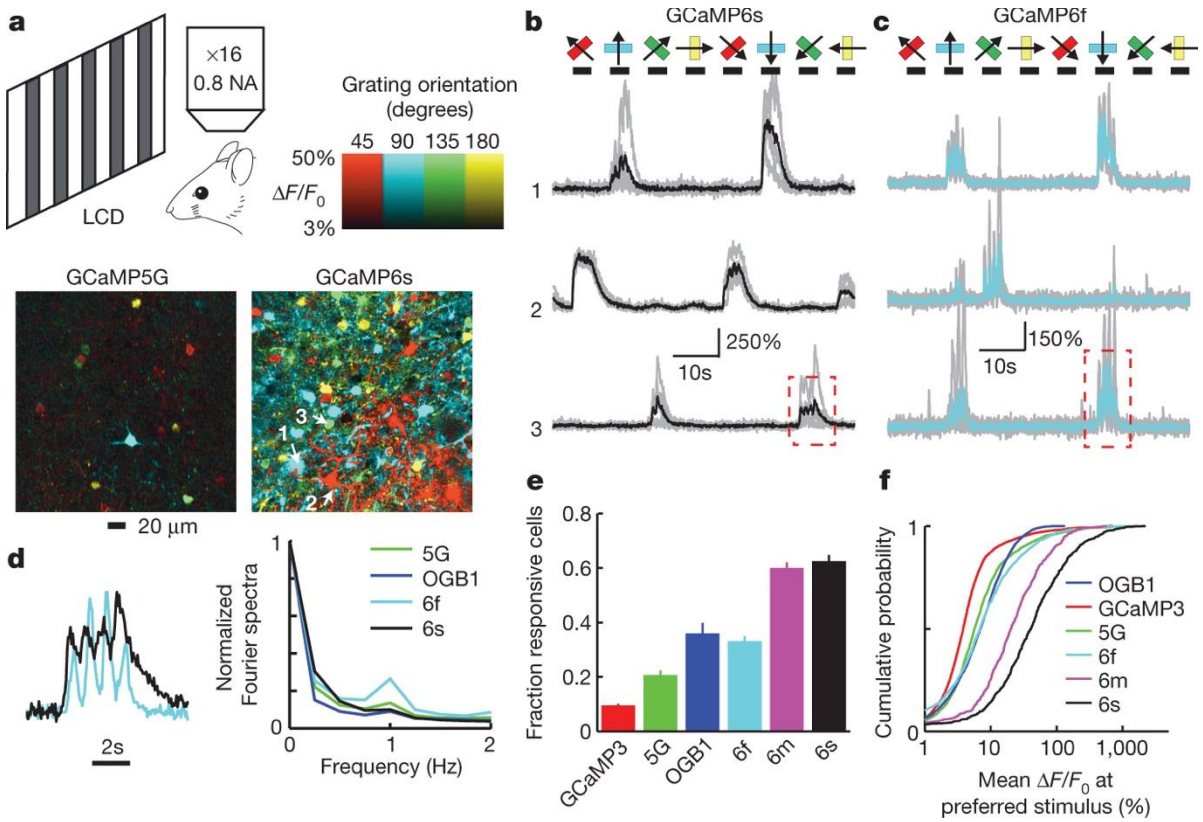

We next tested GCaMP6 in layer (L) 2/3 pyramidal neurons in the mouse visual cortex V1 in vivo. V1 was infected with adeno-associated virus (AAV) expressing GCaMP variants (AAV-hsyn1-GCaMP variant). Three weeks afterAAV infection, the vast majority of L2/3 neurons showed fluorescence mainly in the neuronal cytoplasm

GCaMP6 performance in the mouse visual cortex.

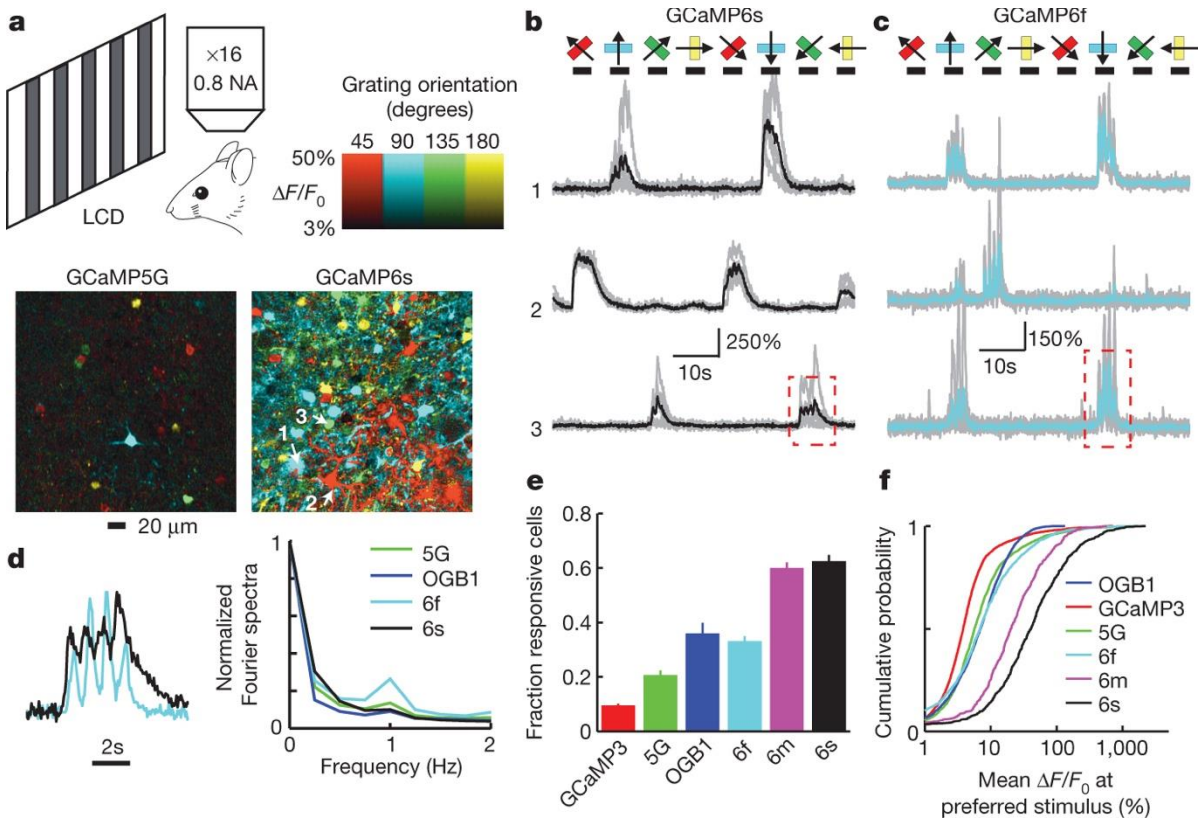

Sensory stimuli consisted of moving gratings presented in eight directions to the contralateral eye. Two-photon imaging revealed visual stimulus-evoked fluorescence transients in subsets of neurons (Fig. 2a–c). Fluorescence transients were faster with GCaMP6f compared to other sensors and faithfully tracked dynamic sensory stimuli (Fig. 2d).

GCaMP6 performance in the mouse visual cortex.

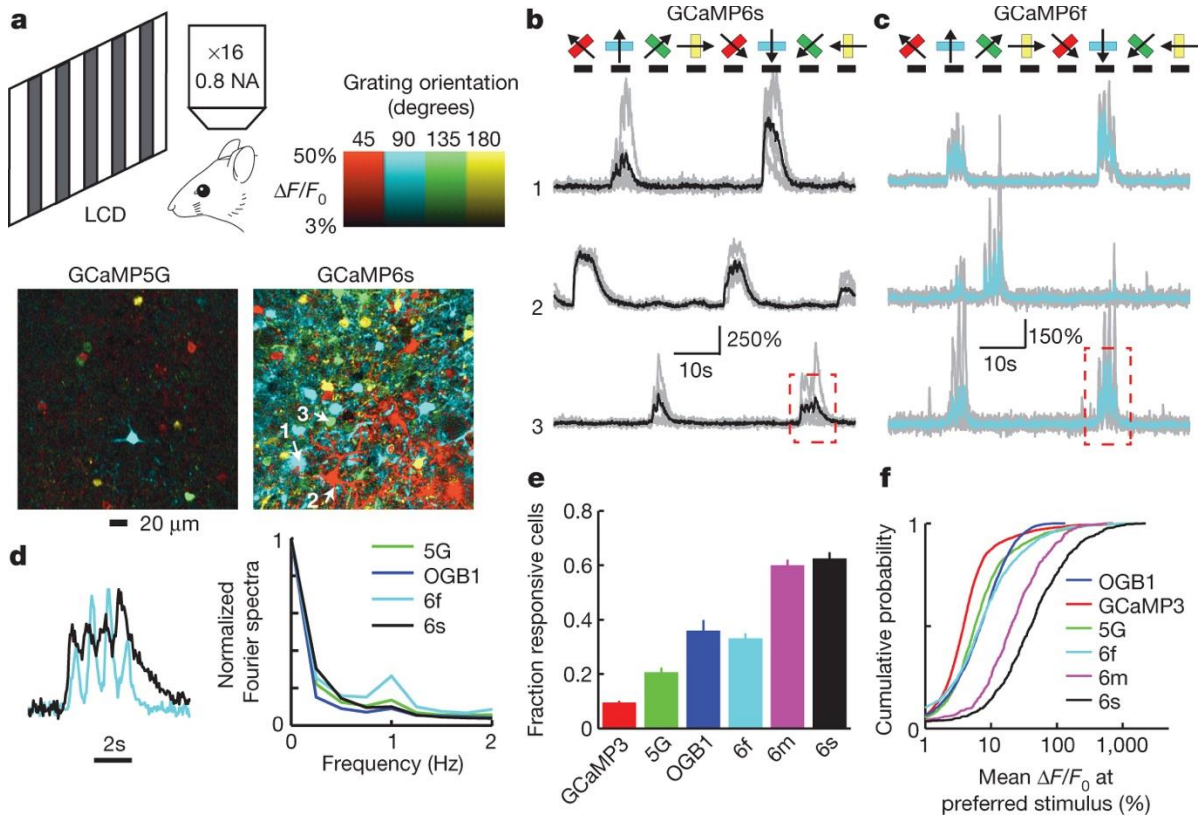

GCaMP6 performance was compared to other sensors in several ways.
The fraction of responding neurons detected with GCaMP6s was threefold higher than for GCaMP5G (fivefold higher than GCaMP3) (Fig. 2e). Notably, the fractions of active neurons detected with GCaMP6s and GCaMP6m were also significantly higher than for OGB1-AM (Fig. 2e, f, P,0.01, Wilcoxon rank sum test).

Combined imaging and electrophysiology in the visual cortex.

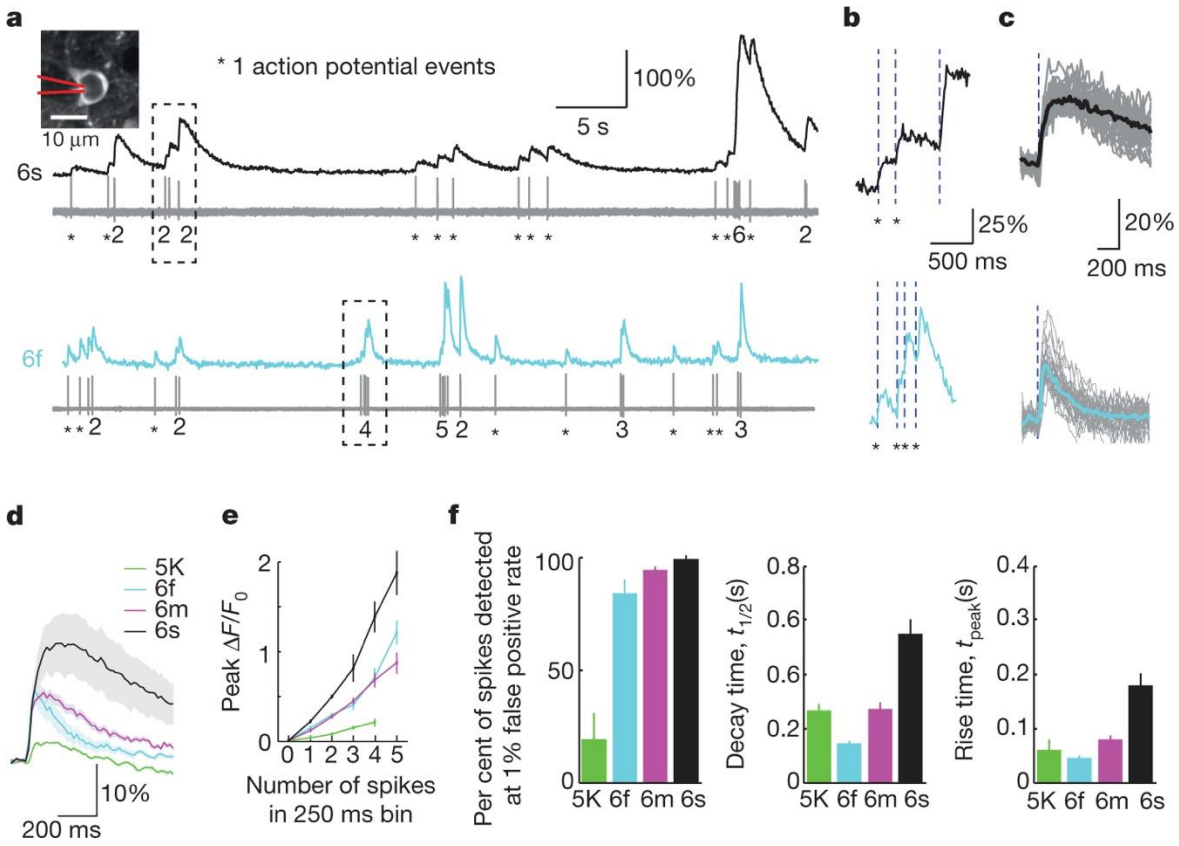

GCaMP6 sensors thus reveal neuronal dynamics that were previously undetectable with protein sensors.

Combined imaging and electrophysiology in the visual cortex.

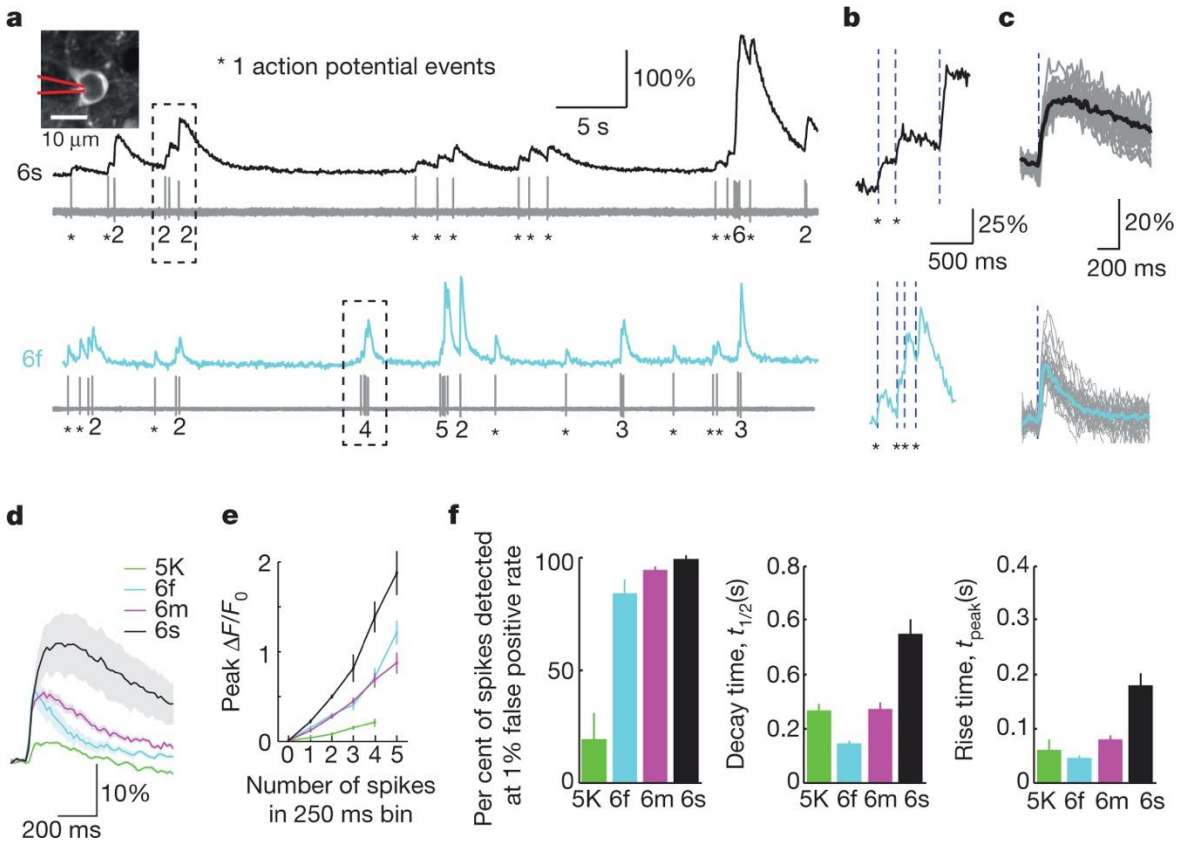

We directly compared cellular fluorescence changes and spiking using loose-seal, cell-attached recordings. GCaMP6s produced large fluorescence transients even in response to single action potentials (.6 times larger than for GCaMP5K, Fig. 3 and Supplementary Video 1), yielding high detection rates for single spikes.

Combined imaging and electrophysiology in the visual cortex.

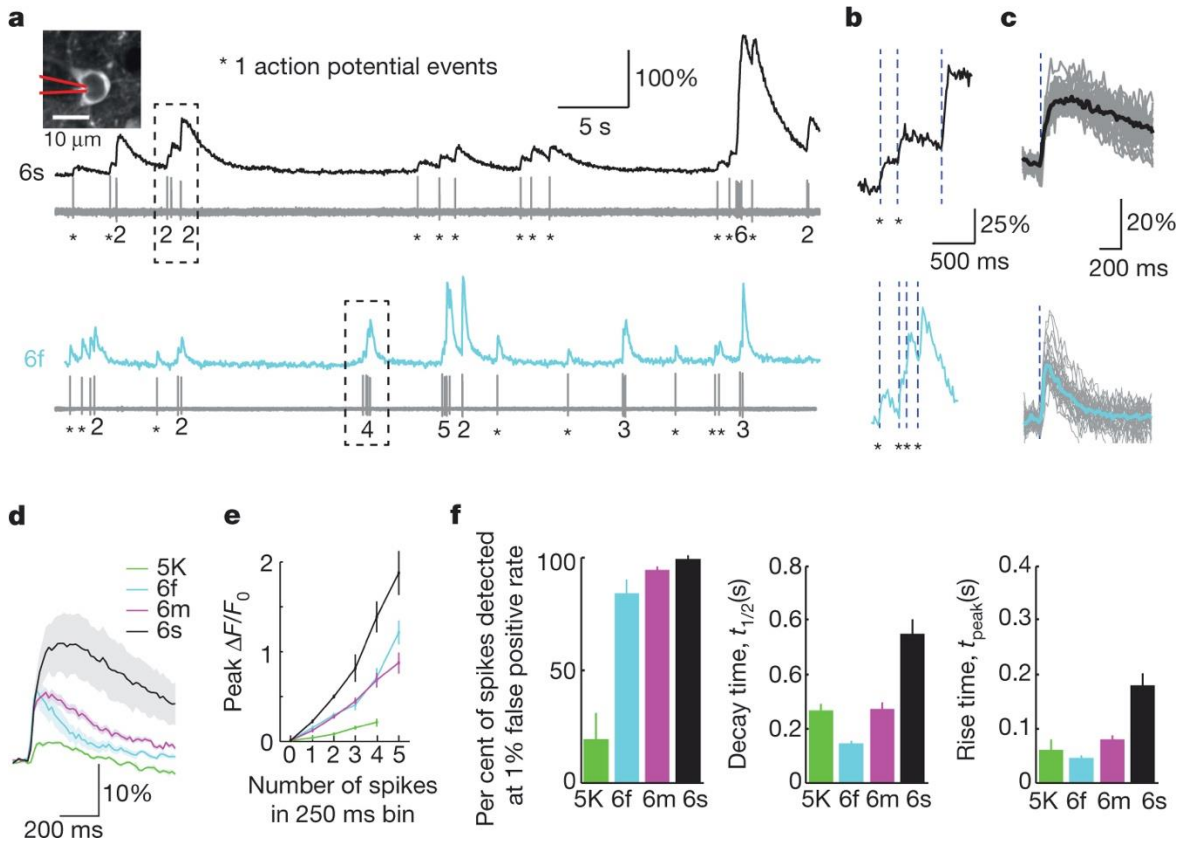

GCaMP6f and GCaMP6m showed slightly lower spike detection efficiencies, but with faster kinetics (Fig. 3). Individual spikes within a burst resulted in stepwise fluorescence increases (Fig. 3b), which were resolvable if they were separated by an interval on the order of the rise time of the sensor or more (100–150ms, GCaMP6s; 75–100 ms, GCaMP6m; 50–75ms, GCaMP6f).


20%
0.5mV
1s
10 µm

GCaMP6 indicators cross important performance thresholds. They have higher sensitivity than commonly used synthetic calcium dyes (for example, OGB1-AM) and detect individual action potentials with high reliability at reasonable microscope magnifications. These indicators can be used to image large groups of neurons as well as tiny synaptic compartments over multiple imaging sessions separated by months. It is likely that these sensors will find widespread applications for diverse problems in brain research and calcium signalling.

Neuron
NeuroResource

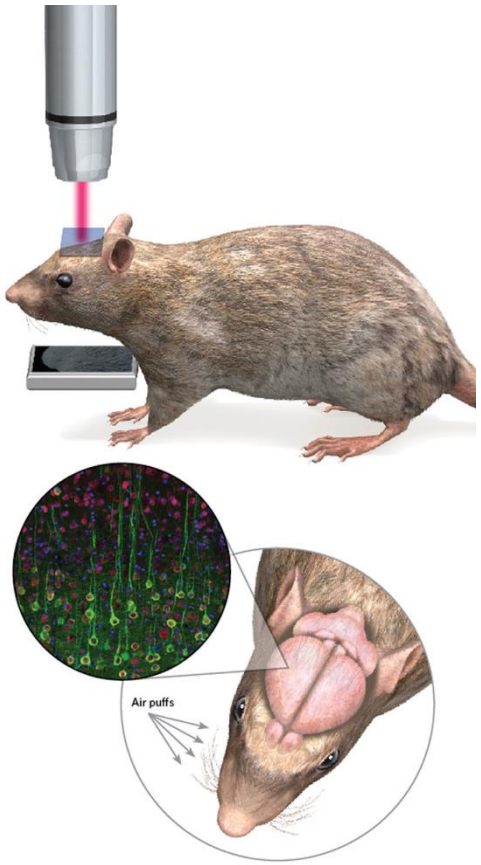

Imaging Neural Activity Using *Thy1*-GCaMP Transgenic Mice

Qian Chen,[1] Joseph Cichon,[3,10] Wenting Wang,[1,10] Li Qiu,[4] Seok-Jin R. Lee,[4] Nolan R. Campbell,[1] Nicholas DeStefino,[6] Michael J. Goard,[2] Zhanyan Fu,[1,5] Ryohei Yasuda,[4] Loren L. Looger,[7] Benjamin R. Arenkiel,[8] Wen-Biao Gan,[3] and Guoping Feng[1,9,*]

[1]McGovern Institute for Brain Research, Department of Brain and Cognitive Sciences
[2]Picower Institute for Learning and Memory, Department of Brain and Cognitive Sciences
Massachusetts Institute of Technology, Cambridge, MA 02139, USA
[3]Molecular Neurobiology Program, Skirball Institute, Department of Physiology and Neuroscience, New York University School of Medicine, New York, NY 10016, USA
[4]Department of Neurobiology
[5]Department of Psychiatry and Behavioral Science
Duke University Medical Center, Durham, NC 27710, USA
[6]MD-PhD Program, Harvard Medical School, Boston, MA 02115, USA
[7]Howard Hughes Medical Institute, Janelia Farm Research Campus, Ashburn, VA 20147, USA
[8]Department of Molecular and Human Genetics, Baylor College of Medicine, Houston, TX 77030, USA
[9]Stanley Center for Psychiatric Research, Broad Institute, Cambridge, MA 02142, USA
[10]These authors contributed equally to this work
*Correspondence: fengg@mit.edu
http://dx.doi.org/10.1016/j.neuron.2012.07.011

PROTEIC fluorescent Ca^{2+} probes

or Genetically Encoded Ca^{2+} Indicators (**GECI**)

Probe	Origin	Detection technique	Ref.
Aequorin	Genetically encoded	Luminometry	15
Berovin	Genetically encoded	Luminometry	22
Obelin	Genetically encoded	Luminometry	23
Cameleon	Genetically encoded	FRET microscopy	24
Troponin C biosensor	Genetically encoded	FRET microscopy	25
Camgaroo	Genetically encoded	Fluorescence microscopy	26
Ratiometric Pericam	Genetically encoded	Ratiometric fluorescence microscopy	27
GEM-GECO1	Genetically encoded	Ratiometric fluorescence microscopy	28
Calcium Green-1	Synthetic	Fluorescence microscopy	29
Fluo-3, Fluo-4	Synthetic	Fluorescence microscopy	29
Fura-2, Indo-1	Synthetic	Ratiometric fluorescence microscopy	30

Bonora M. et al., 2013 *Nature Proocols*

AEQUORIN

Aequorea victoria (Jellyfish)

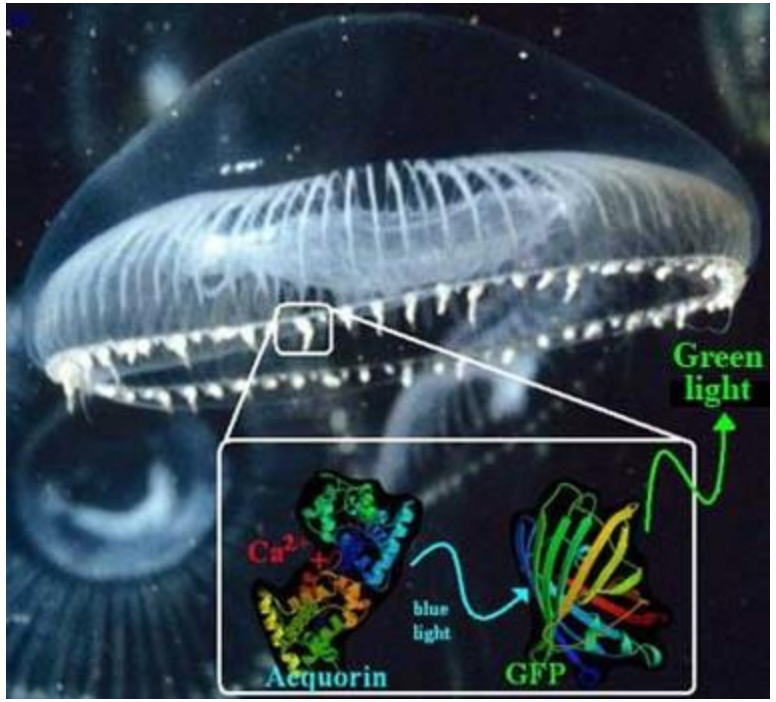

PROTEIC fluorescent Ca^{2+} probes

AEQUORIN

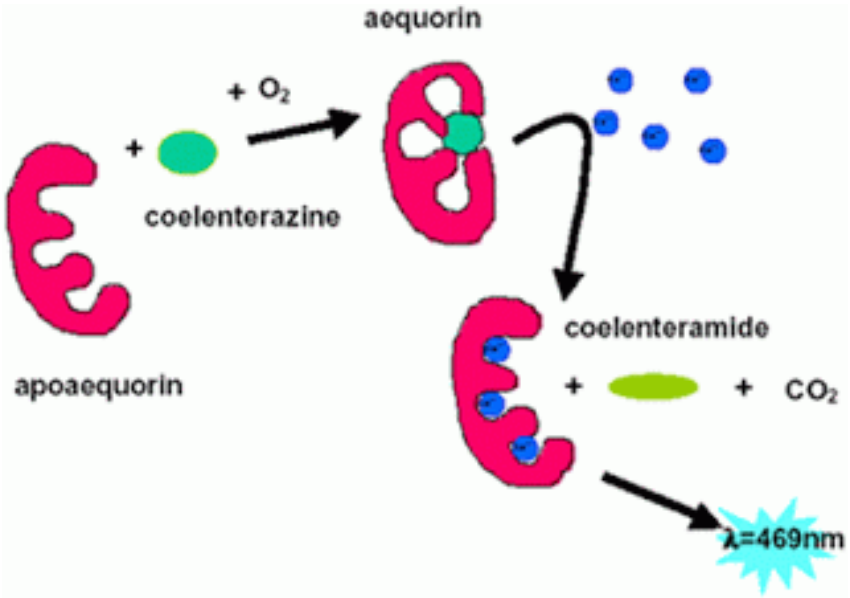

- In the active form: the protein includes a prosthetic group (coelenterazine) that is oxidezed and released in the Ca^{2+}-triggered reaction.
- Binds Ca^{2+} to three high-affinity sites
- Irreversible reaction with a photon emission (λ_{em}: 470nm)

AEQUORIN

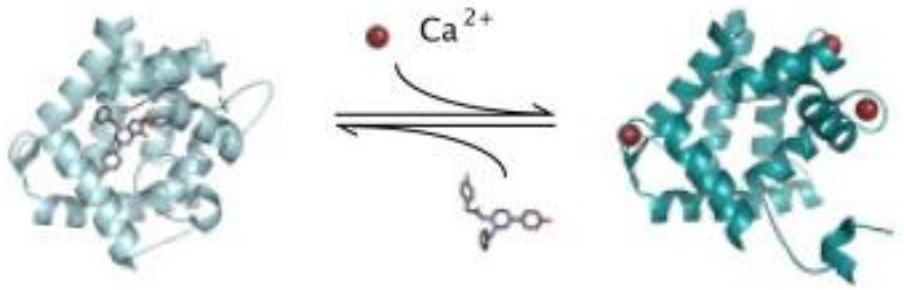

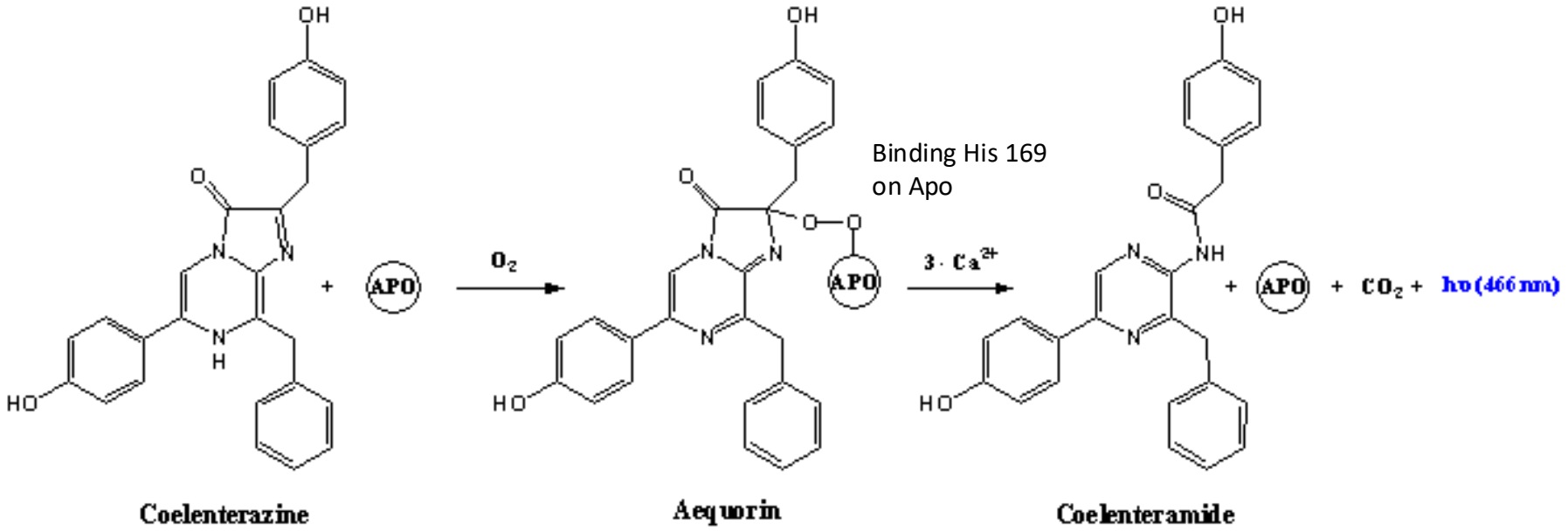

Coelenterazine

Aequorin

Coelenteramide

PROTEIC fluorescent Ca^{2+} probes

Department of
Life Sciences
and Systems Biology

AEQUORIN

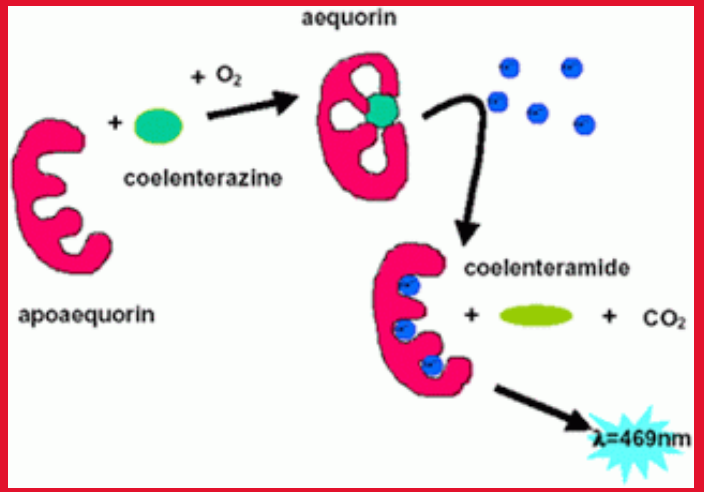

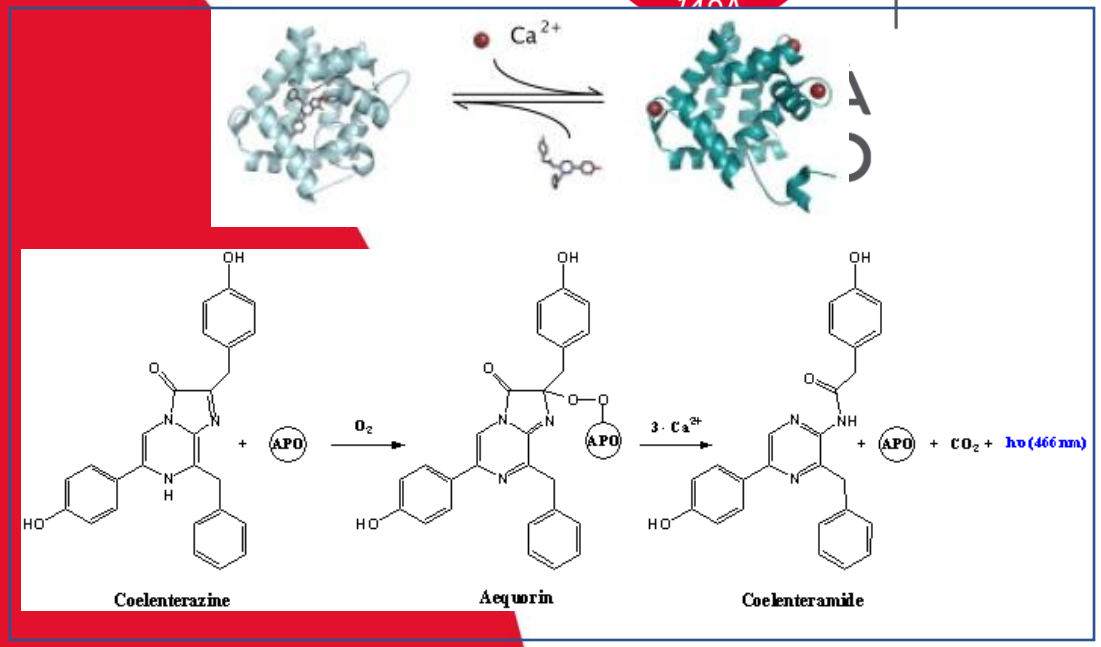

PROBE RECONSTITUTION

The expression of aequorin cDNA yields the polypeptide, to which the prosthetic group must be added.

Coelenterazine is highly hydrophobic and, when added to the culture medium of aequorin-expressing cells, will freely permeate through the cell membrane. Once inside the cell, coelenterazine, generating the active probe.

PROTEIC fluorescent Ca^{2+} probes

AEQUORIN

how to measure $[Ca^{2+}]$

a

$$Ca^{2+}\,(M) = \frac{\left(\frac{L}{L_{max}} \times \lambda\right)^{\frac{1}{n}} + \left(\left(\frac{L}{L_{max}} \times \lambda\right)^{\frac{1}{n}} \times K_{TR}\right) - 1}{K_R - \left(\left(\frac{L}{L_{max}} \times \lambda\right)^{\frac{1}{n}} \times K_R\right)}$$

L = light intensity at sampling time

L_{max} = total light emitted at sampling time ✶

K_R = constant for calcium-bound state

K_{TR} = constant for calcium-unbound state

λ = rate constant for aequorin consumption at saturating $[Ca^{2+}]$

n = number of Ca^{2+}-binding site

✶L_{max} is the maximal rate of discharge at saturating $[Ca^{2+}]$

There is a relationship between the fractional rate of consumption (L/L_{max}) and $[Ca^{2+}]$

b

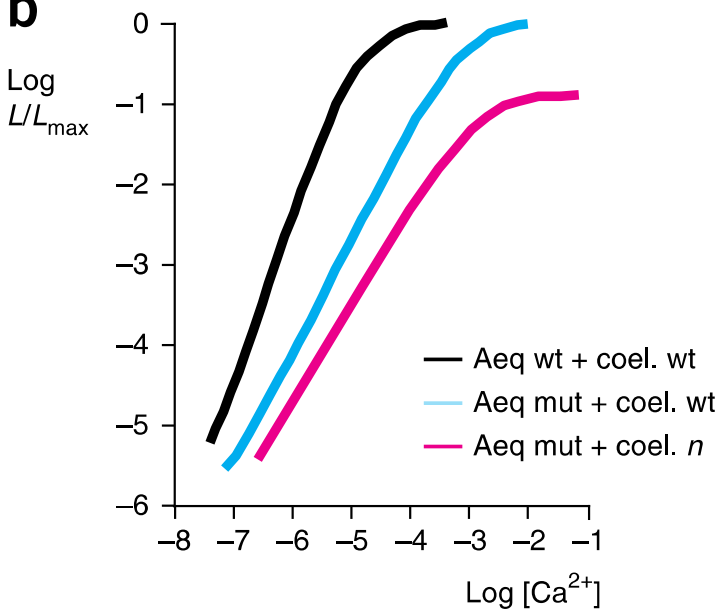

PROTEIC fluorescent Ca^{2+} probes

AEQUORIN

Owing to cooperation between the three binding sites, light emission is proportional to the second to third power of [Ca^{2+}]

→ on the one hand accounts for the excellent S/N ratio of aequorin

→ on the other hand may subtantially affect the measurements

Given that the probe (differently from fluorescent indicators) is **gradually consumed** throughout the experiment, the signal tends to decrease, and the conversion into [Ca^{2+}] concentration can be obtained only at the end of the experiment, when, after cell lysis, the total aequorin content is estimated and L/L_{max} can be back calculated for each data point.

PROTEIC fluorescent Ca^{2+} probes

AEQUORIN

Major advantages of using aequorin

1) high signal-to-noise (S/N) ratio

background of aequorin measurement is very low because mammalian cells doesn't express chemiluminescent proteins

↓

i.e. upon stimulation of cells a 1,000–10,000-fold over background signals can be detected, respectively with cytosolic and mitochondrial aequorin.

Because of the excellent S/N ratio, reliable aequorin measurements can be obtained with moderate levels of expression of the probe.

PROTEIC fluorescent Ca^{2+} probes

AEQUORIN

Major advantages of using aequorin

2) selective intracellular distribution

The main reason for the renewed interest in using aequorin is that, being a protein, it can be engineered to induce its specific localization to a cell region of interest.

cytAEQ → wild-type cytosolic aequorin

the addition of specific targeting sequences permits selective localization of the photoprotein, resulting in recombinant aequorin chimeras for different intracellular compartments:

nuAEQ → nucleus
mtAEQ and **mimsAEQ** → mitochondria
pmAEQ → subplasma-membrane cytosol
erAEQ/srAEQ → endoplasmic/sarcoplasmic reticulum
goAEQ → golgi apparatus
vampAEQ → secretory vesicles
peroxAEQ → peroxisomes

TABLE 2 | Description of the compartment-specific aequorin chimeras available.

Intracellular localization	Acronym	Targeting strategy
Cytosol	CytAEQ	No targeting sequence is added to aequorin; the sequence of aequorin was modified only by adding the epitope tag HA1 (ref. 15)
Nucleus	NuAEQ	A fragment of rat glucocorticoid receptor, lacking the hormone-binding domain and the nuclear localization signal are fused with the HA1-tagged aequorin[31]
	MtAEQwt	Mitochondrial pre-sequence of subunit VIII of cytocrome *c* oxidase (COX) is fused to the HA1-tagged aequorin, for measurements of $[Ca^{2+}]$ up to 10–15 μM (ref. 32)
Mitochondrial matrix	mtAEQmut	The mutated version of mtAEQwt. Because of the cooperativity between the three Ca^{2+}-binding sites of aequorin, the point mutation (Asp119Ala)[13] that affects the second EF-hand domain, produces a mutated aequorin, which can be used to measure $[Ca^{2+}]$ in the range of 10–500 μM (ref. 33)
	mtAEQmut28,119	Double-mutated form (Asp119Ala and Asn28Leu) of mtAEQwt, which can be used to measure $[Ca^{2+}]$ in the millimolar range for long periods of time, without problems derived from aequorin consumption[14]
Mitochondrial intermembrane space	MimsAEQ	HA1-tagged aequorin is fused (sequence in frame) with glycerol phosphate dehydrogenase, an integral protein of the inner mitochondrial membrane, with a large C-terminal tail protruding on the outer side of the membrane, i.e., in the mitochondrial intermembrane space[34]
Plasma membrane	pmAEQ	The targeting of aequorin to the subplasmalemmal space was based on the construction of a fusion protein including the HA1-tagged aequorin and SNAP-25, a protein that is synthesized on free ribosomes and recruited to the inner surface of the plasma membrane after the palmitoylation of specific cysteine residues[35]
Endoplasmic reticulum	erAEQmut	The encoded polypeptide includes the leader sequence (L), the VDJ and CH1 domains of an Igg2b heavy chain (HC) and the HA1-tagged aequorin at the C-terminus. In this chimera, retention in the ER depends on the presence of the CH1 domain at the N terminus of aequorin. This domain is known to interact with the luminal ER protein BiP, thus causing the retention of the Igg2b HC in the lumen. In the absence of the immunoglobulin light chain, the polypeptide is retained in this compartment[36]
Sarcoplasmic reticulum	srAEQmut	Calsequestrin (CSQ), a resident protein of the sarcoplasmic reticulum, is fused to HA1-tagged aequorin. This chimera is used to measure $[Ca^{2+}]$ in the sarcoplasmic reticulum, the specialized muscle compartment involved in the regulation of Ca^{2+} homeostasis[37]
Golgi apparatus	goAEQmut	Fusion of the HA1-tagged aequorin and the transmembrane portion of sialyltransferase, a resident protein of the Golgi lumen[18]
Secretory vescicles	vampAEQmut	Mutated AEQ (AEQmut; Asp119Ala) is fused to the vesicle-associated membrane protein (vamp)2/synaptobrevin (a vesicle-specific SNARE with a single transmembrane-spanning region) allowing intravesicular $[Ca^{2+}]$ to be monitored[38]
Peroxisomes	peroxAEQ	HA1-tagged wild-type and Asp119Ala mutant aequorins were fused with a peroxisomal targeting sequence[17]

PROTEIC fluorescent Ca^{2+} probes

Major advantages of using aequorin

3) low buffering effect on intracellular Ca^{2+}

Aequorin displays an extremely low buffering effect on intracellular Ca^{2+} if compared with fluorescent Ca^{2+} indicators.

Example:
Fura-2 measurements in the presence or absence of aequorin display the same cytoplasmic Ca^{2+} levels; on the contrary, aequorin measurements show a strong reduction in cytoplasmic [Ca^{2+}] if Fura-2 is added.

PROTEIC fluorescent Ca^{2+} probes

AEQUORIN

Major advantages of using aequorin

4) wide dynamic range

Native aequorin and its mutants are well suited for measuring:

0.1 µM < [Ca^{2+}] < **mM** range

Numerous chemical modifications of the prosthetic group modify, in different ways, the Ca^{2+}-triggered reaction of the photoprotein. Among these:

- Those resulting in lower light emission at high [Ca^{2+}] and lower Ca^{2+} affinity → allow measurements at higher [Ca^{2+}] (i.e. Golgi, ER, peroxisomes or mitochondria in certain cell types)

- Those resulting in higher light emission and higher Ca^{2+} affinity → allowing measurements in compartments with low [Ca^{2+}] (i.e. cytoplasm or mithocondria in other cells)

PROTEIC fluorescent Ca^{2+} probes

AEQUORIN

Major disadvantages of using aequorin

1) low light emission by the photoprotein

Only one photon can be emitted by an aequorin molecule and only a small fraction of the total aequorin pool emits its photon every second. This means that out of the 10^4–10^5 molecules per cell of a typical aequorin transfection, light emission will vary from 0 to 1,000 photons at most

The experiments should be conducted NOT on single cell but on entire cell populations → measurments of [Ca^{2+}] represent the average of the signals in that populations

PROTEIC fluorescent Ca^{2+} probes

AEQUORIN

Major disadvantages of using aequorin

2) overestimation of the average rise in cells (or compartments) with non-homogeneous behavior

if the probe is distributed between an high-Ca^{2+} and a low-Ca^{2+} domain, the total signal will be calibrated as 'average' [Ca^{2+}] increase, which will be severely biased by the region with high Ca^{2+} !!! → overestimation

3) cells must be amenable to transfection

The obvious requirement of this approach is that the cell type being studied must be amenable to transfection.

PROTEIC fluorescent Ca^{2+} probes

AEQUORIN

Set up

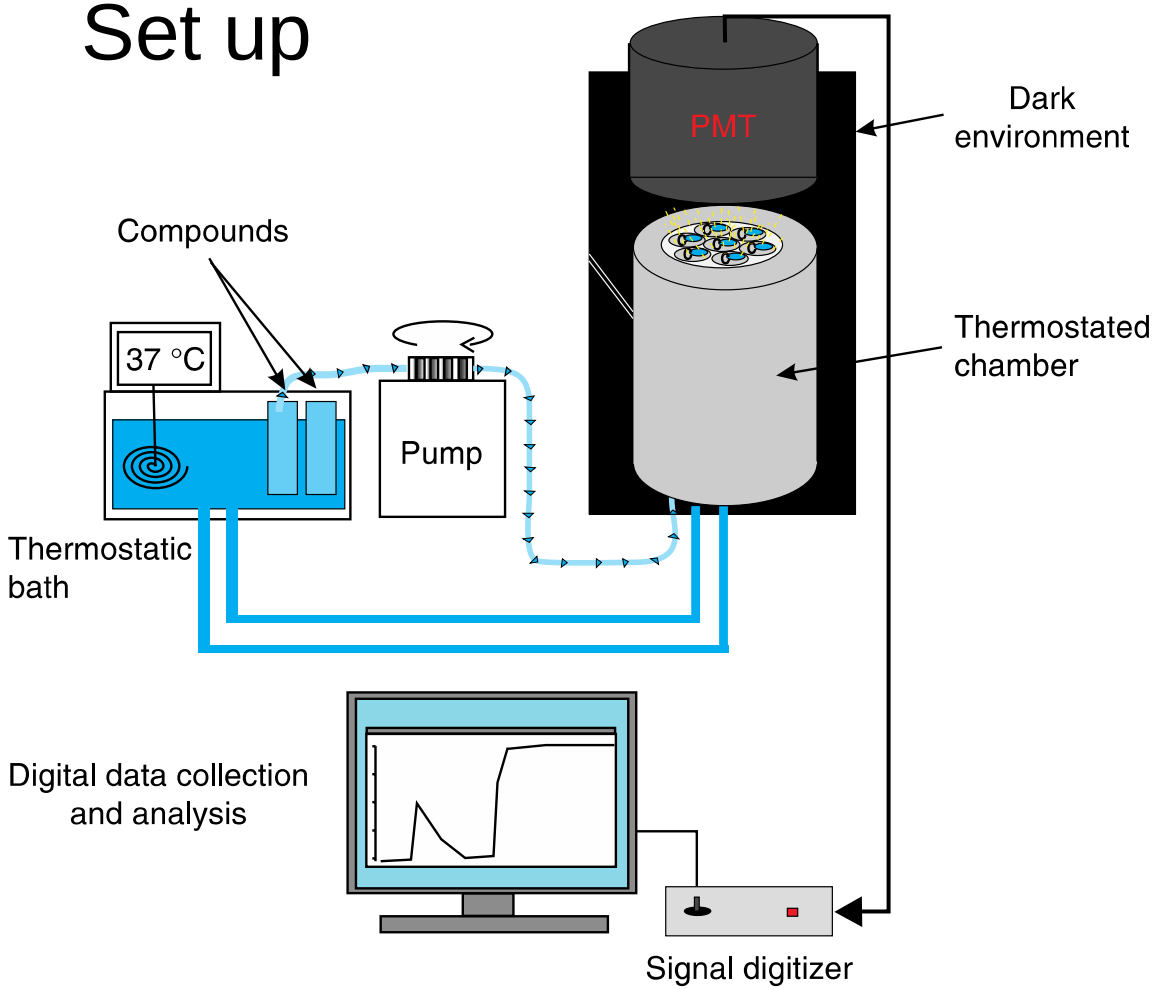

PROTEIC fluorescent Ca^{2+} probes

AEQUORIN

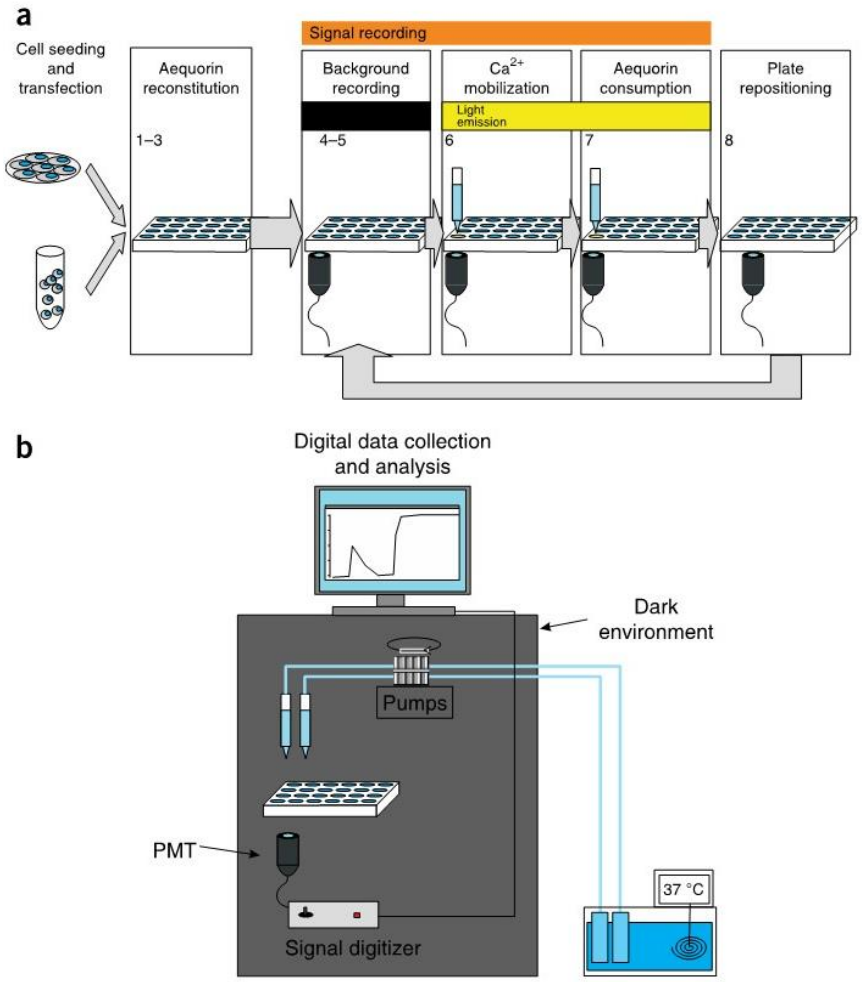

Bonora M. et al., 2013 *Nature Protocols*

Set up for high throughput assays

Possibility to perform the experiment on:

automated 96-well plate reader luminometers plate

(reduced sensitivity)

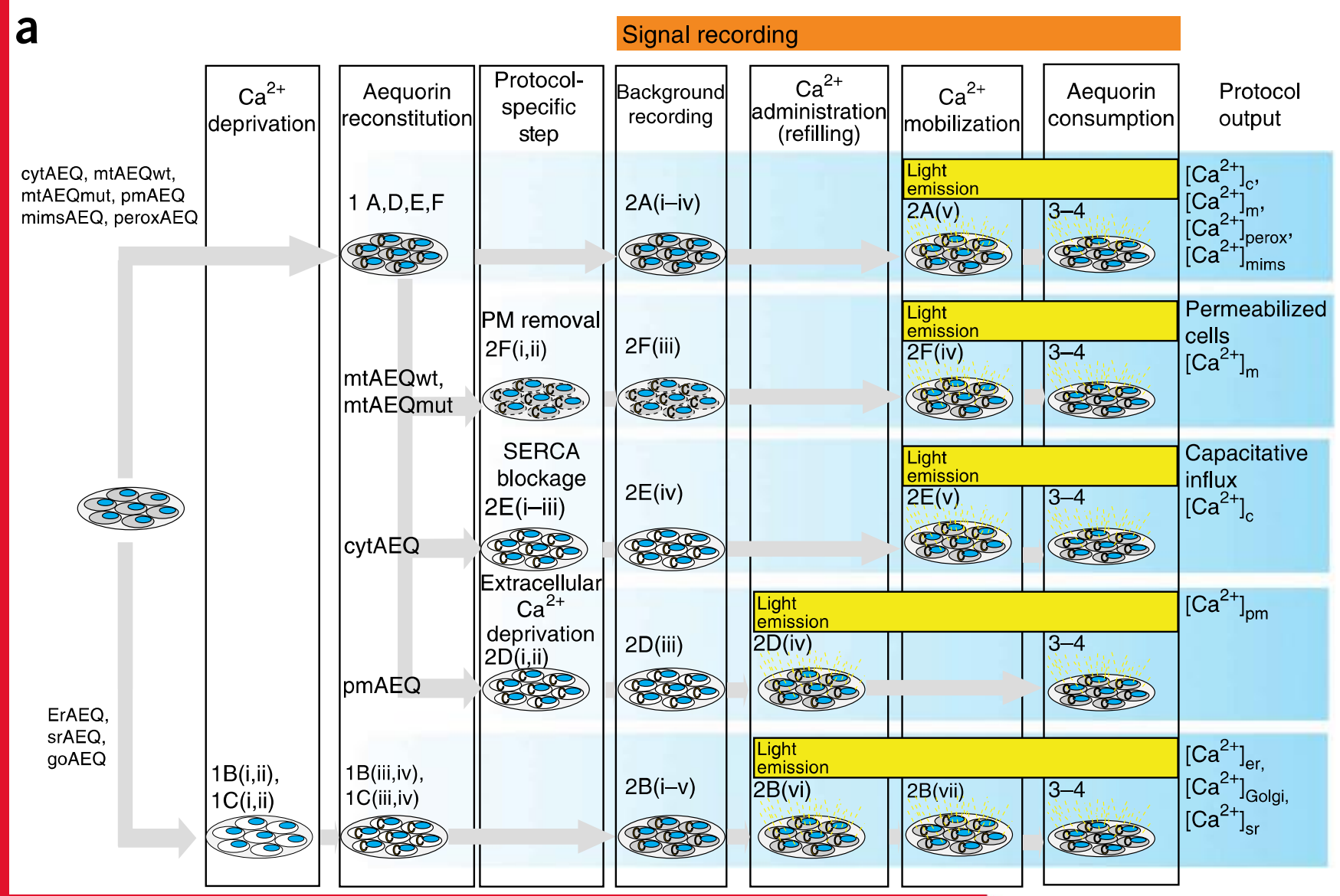
a
Signal recording
Ca2+ deprivation
Aequorin reconstitution
Protocol-specific step
Background recording
Ca2+ administration (refilling)
Ca2+ mobilization
Aequorin consumption
Protocol output
cytAEQ, mtAEQwt, mtAEQmut, pmAEQ mimsAEQ, peroxAEQ
1 A,D,E,F
2A(i–iv)
Light emission
2A(v)
3–4
[Ca2+]c, [Ca2+]m, [Ca2+]perox, [Ca2+]mims
PM removal 2F(i,ii)
2F(iii)
mtAEQwt, mtAEQmut
Light emission
2F(iv)
3–4
Permeabilized cells [Ca2+]m
SERCA blockage 2E(i–iii)
2E(iv)
cytAEQ
Light emission
2E(v)
3–4
Capacitative influx [Ca2+]c
Extracellular Ca2+ deprivation 2D(i,ii)
2D(iii)
pmAEQ
Light emission
2D(iv)
3–4
[Ca2+]pm
ErAEQ, srAEQ, goAEQ
1B(i,ii), 1C(i,ii)
1B(iii,iv), 1C(iii,iv)
2B(i–v)
Light emission
2B(vi)
2B(vii)
3–4
[Ca2+]er, [Ca2+]Golgi, [Ca2+]sr

PROTEIC fluorescent Ca^{2+} probes

AEQUORIN

appropriate CONTROLS

- ✓ A **positive control** for probe expression is provided by **cell lysis**, which is done as the final phase of each procedure. Light emission induced upon cell lysis is directly proportional to the whole amount of aequorin expression.

- ✓ A useful **negative control** is to perform the preferred reconstitution and recording procedure in **non transfected cells**

PROTEIC fluorescent Ca^{2+} probes

or Genetically Encoded Ca^{2+} Indicators (**GECI**)

Probe	Origin	Detection technique	Ref.
Aequorin	Genetically encoded	Luminometry	15
Berovin	Genetically encoded	Luminometry	22
Obelin	Genetically encoded	Luminometry	23
Cameleon	Genetically encoded	FRET microscopy	24
Troponin C biosensor	Genetically encoded	FRET microscopy	25
Camgaroo	Genetically encoded	Fluorescence microscopy	26
Ratiometric Pericam	Genetically encoded	Ratiometric fluorescence microscopy	27
GEM-GECO1	Genetically encoded	Ratiometric fluorescence microscopy	28
Calcium Green-1	Synthetic	Fluorescence microscopy	29
Fluo-3, Fluo-4	Synthetic	Fluorescence microscopy	29
Fura-2, Indo-1	Synthetic	Ratiometric fluorescence microscopy	30

FRET-tandem probes modified to measure Ca^{2+}

CAMELEON

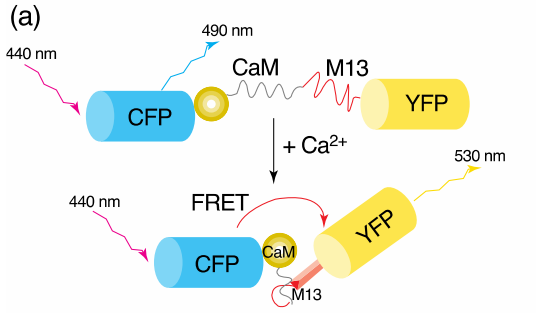

Bonora M. et al., 2013 *Nature Proocols*

PROTEIC fluorescent Ca^{2+} probes

CAMELEON

Cameleons are chimeric proteins consisting of:

- blue or cyan mutant of green fluorescent protein (GFP),
- calmodulin (CaM),
- a glycylglycine linker,
- the CaM-binding domain of myosin light chain kinase (M13),
- and a green or yellow version of GFP.

Ca^{2+} binding to the CaM → intramolecular CaM binding to M13 → more compact conformation → increased efficency of fluoresce resonance energy transfer (FRET)

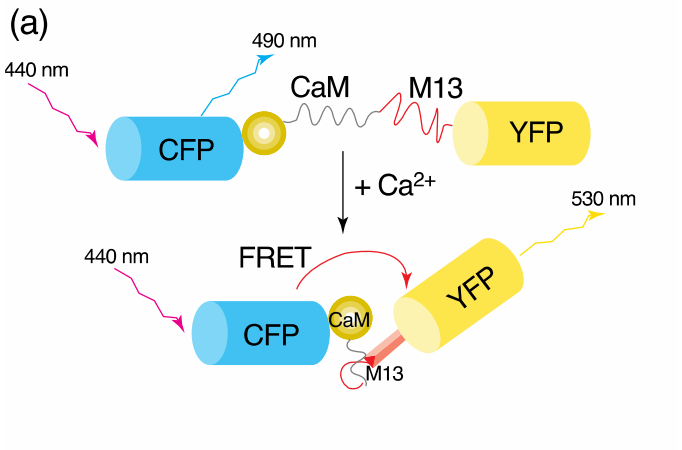

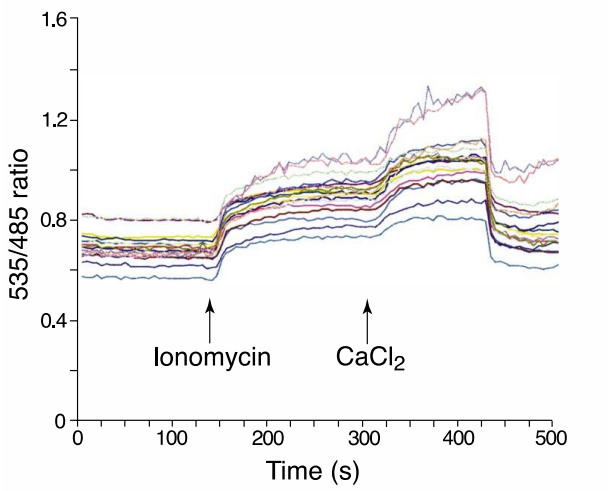

PROTEIC fluorescent Ca^{2+} probes

CAMELEON

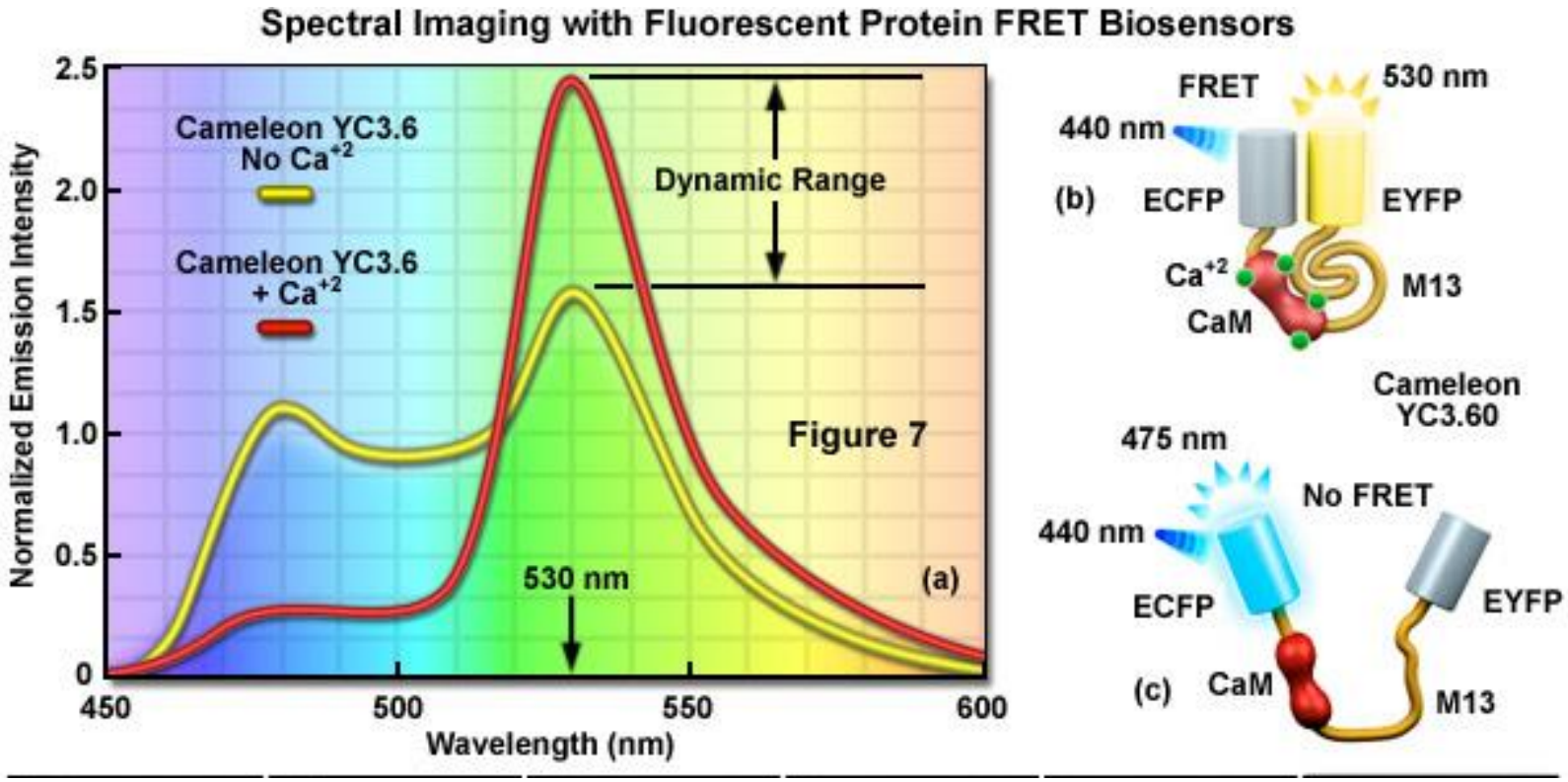

http://zeiss.magnet.fsu.edu/tutorials/spectralimaging/spectralfret/indexflash.html

PROTEIC fluorescent Ca^{2+} probes

CAMELEON

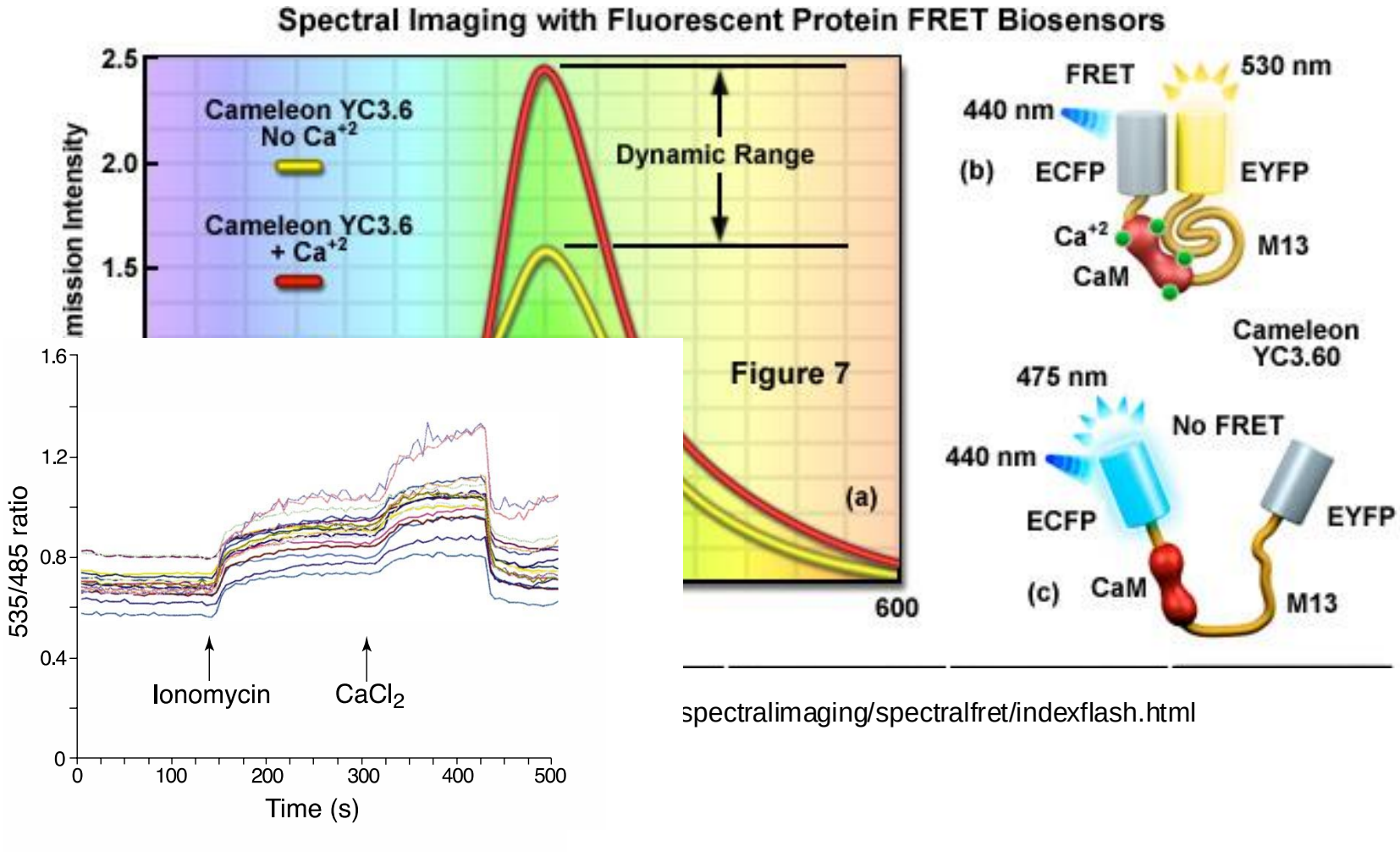

spectralimaging/spectralfret/indexflash.html

UNIVERSITÀ
DI TORINO

Department of
Life Sciences
and Systems Biology

Thank you